RESEARCH ARTICLE • OPEN ACCESS

Mathematical Modeling, Optimal Control and Cost-Effectiveness Analysis of Diphtheria Transmission Dynamics

Ayodeji Sunday Afolabi and Miswanto Miswanto

Volume 6, Issue 2, Pages 88–108, June 2025

Received 11 March 2025, Revised 28 April 2025, Accepted 7 June 2025, Published Online 24 June 2025

To Cite this Article : A. S. Afolabi and M. Miswanto,"Mathematical Modeling, Optimal Control and Cost-Effectiveness Analysis of Diphtheria Transmission Dynamics", *Jambura J. Biomath*, vol. 6, no. 2, pp. 88–108, 2025, *https://doi.org/10.37905/jjbm.v6i2.30851*

JOURNAL INFO • JAMBURA JOURNAL OF BIOMATHEMATICS

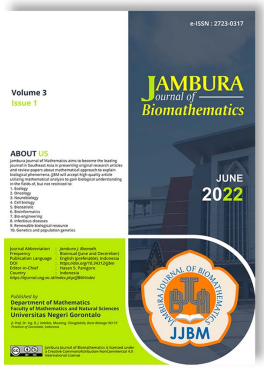

Homepage	:	http://ejurnal.ung.ac.id/index.php/JJBM/index
Journal Abbreviation	:	Jambura J. Biomath.
Frequency	:	Quarterly (March, June, September and December)
Publication Language	:	English
DOI	:	https://doi.org/10.37905/jjbm
Online ISSN	:	2723-0317
Editor-in-Chief	:	Hasan S. Panigoro
Publisher	:	Department of Mathematics, Universitas Negeri Gorontalo
Country	:	Indonesia
OAI Address	:	http://ejurnal.ung.ac.id/index.php/jjbm/oai
Google Scholar ID	:	XzYgeKQAAAAJ
Email	:	editorial.jjbm@ung.ac.id

JAMBURA JOURNAL • FIND OUR OTHER JOURNALS

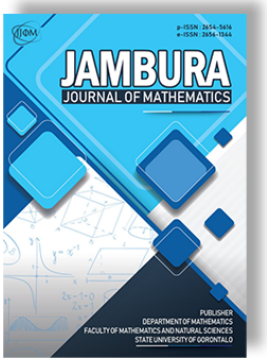

Jambura Journal of Mathematics

Jambura Journal of Mathematics Education

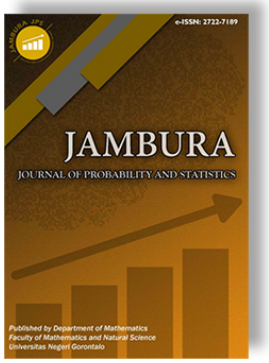

Jambura Journal of Probability and Statistics

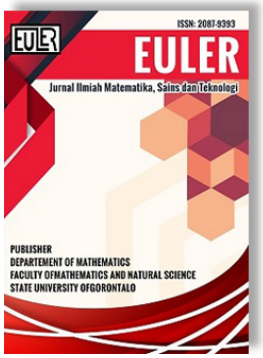

EULER : Jurnal Ilmiah Matematika, Sains, dan Teknologi

Jambura Journal of Biomathematics, Volume 6, Issue 2, Pages 88–108, June 2025 https://doi.org/10.37905/jjbm.v6i2.30851

Research Article

Check for updates

Mathematical Modeling, Optimal Control and Cost-Effectiveness Analysis of Diphtheria Transmission Dynamics

Ayodeji Sunday Afolabi[1] and **Miswanto Miswanto**[2,*]

[1]*Department of Mathematical Sciences, Federal University of Technology, Akure, P.M.B. 704, Akure, Ondo State, Nigeria*
[2]*Department of Mathematics, Faculty of Sciences and Technology, Airlangga University, Surabaya, Indonesia*

ARTICLE HISTORY
Received 11 March 2025
Revised 28 April 2025
Accepted 7 June 2025
Published 24 June 2025

KEYWORDS
Diphtheria
Non-linear
Stability analysis
Sensitivity analysis
Optimal control problem
Cost-effectiveness analysis

ABSTRACT. *Diphtheria remains a serious public health concern in regions with low vaccination coverage and limited access to timely treatment, highlighting the urgent need for effective modeling and control strategies to guide intervention efforts. A nonlinear mathematical model is developed to describe the transmission dynamics of diphtheria. The well-posedness of the model is analyzed by investigating the positivity and boundedness of its solutions. The solutions of the disease-free equilibrium points are obtained analytically. The basic reproduction number ($\mathbb{R}_0$) is determined using Diekmann-Heesterbeek-Metz Next Generation Matrix approach. The stability of the disease-free and endemic equilibrium points are rigorously analyzed. Sensitivity analysis of the model parameters with respect to $\mathbb{R}_0$ is conducted to assess the relative impact of each parameter on the transmission dynamics of the disease. Based on the results of the sensitivity analysis, the proposed diphtheria model is extended into an optimal control problem by introducing four time-dependent control variables: personal protection, booster vaccine administration, detection/treatment of the asymptomatic infected humans and reduction of bacteria concentration. Four different scenarios with each involving at least three of the control variables are examined. We evaluated the cost-effectiveness of each control strategy using IAR, ACER and ICER methods in order to identify the most economically efficient strategy. The findings demonstrate that Strategy A is the most cost-effective startegy that can significantly reduce diphtheria transmission throught optimal personal protection, detection/treatment of the asymptomatic infected humans and reduction of bacteria concentration.*

1. Introduction

Diphtheria is a highly contagious disease caused by specific strains of the bacterium Corynebacterium diphtheriae that produce a harmful toxin. This toxin can lead to severe respiratory issues and other complications if left untreated. Infected individuals become very sick due to the presence of this toxin in the throat, upper airways and other organs of the body. The diphtheria toxin makes breathing very difficult by building up a layer of dead tissue form over the throat and tonsils. The symptoms of the disease include low fever, sore throat and swollen glands in the neck. It is worth noting that a total of 27,991 suspected cases of diphtheria with 828 deaths have been recorded in Guinea, Mauritania, Niger, Nigeria and South Africa as at 14th January, 2024. Out of this number, Nigeria account for 80.1% and 72% of the suspected cases and fatalities respectively. Diphtheria is a vaccine-preventable disease that is highly contagious. The disease spreads between humans through direct contact or respiratory droplets in the air. It is potentially fatal and can lead to death within few days. Diphtheria is primarily transmitted via direct physical contact or through respiratory droplets expelled during coughing or sneezing or coughs of infected humans by breathing in the secretions released into the air. Individuals of all age groups can contract the disease by coming in contact with infected open sores. However, children who are not immunized against the disease are at higher risks of contracting the disease. In addition to these, people living or staying in the same household with individuals that have come in close contact with or secretions from infected people or objects are at higher risk [1].

Over the years, many researchers have worked on mathematical models for the control of diphtheria [2–13]. Madubueze [14] formulated a mathematical model for the transmission dynamics and control of diphtheria and incorporated vaccine booster and contaminated environment into the dynamics of the disease. Latin Hypercube Sampling (LHS) was adopted to calculate the global stability of the polluted environment and infected individuals. Hence, these techniques enabled the authors to obtain the sensitive parameters that had the most significant effects on the transmission dynamics of the disease. Based on thess results, the model was expanded into an optimal control problem (OCP) by incorporating four time-dependent control variables - screening, disinfection, hygienic practice and booster vaccination. Pontryagin's Maximum Principle was employed to derive the necessary conditions for optimality of the control problem

*Corresponding Author.

Email : *miswanto@fst.unair.ac.id* (M. Miswanto)
Homepage : http://ejurnal.ung.ac.id/index.php/JJBM/index / E-ISSN : 2723-0317

and the numerical simulation revealed that the disease would be curtailed by implementing a number of these control measures.

A mathematical model was developed to describe and analyze the transmission dynamics of diphtheria, capturing the interactions between key epidemiological compartments. The model incorporated different movements among the classes and the need for constant hand-washing. The results revealed that there were - disease free and endemic equilibria. It was established that if $\mathbb{R}_0 < 1$, the disease free equilibrium was stable and that there existed an endemic equilibrium state if $\mathbb{R}_0 > 1$. The findings showed that increasing the rate of vaccination, putting infected people in a quarantine and constant hand-washing behaviour among infected individuals would significantly reduce $\mathbb{R}_0$ [15]. Medugu [16] asserted that Corynebacterium diphtheriae was the major cause of endemic and epidemic diphtheria. The delivery and efficacy of modern vaccines deplored to tackle 2023 outbreaks of diphtheria and failure to immunize during childhood were investigated.

An age-structured model was formulated and analyzed to study the epidemiological modeling of the spread of diphtheria infection. The mathematical analysis of the model revealed that the model was epidemiologically meaningful and that when $\mathbb{R}_0 < 1$, the system was globally asymptotically stable (GAS) [17]. Real-time analyses on mathematical models for the transmission dynamics of diphtheria in Bangladesh were conducted. The feedback of major information about the dynamics of the disease at a point when information on the mode of transmission of the disease and its prevalence was largely unknown [18]. Islam [19] formulated a deterministic mathematical model for diphtheria outbreaks in Bangladesh, Rohingya refugee camp in order to understand the disease dynamics. The authors obtained the analytical and numerical solutions of the model's compartments. The results revealed the positivity and boundedness of the solutions, as well as the identification of the disease's persistence and extinction equilibria within the model. Numerical techniques were used to estimate the parameter values from the record of daily cases of the disease. For this specific outbreak, $\mathbb{R}_0$ was calculated to be 5.86.

A mathematical model was constructed to evaluate control strategies for diphtheria infection, incorporating a natural immunity rate for individuals exposed to the disease. From the numerical simulation, it was discovered that the total immunization coverage and the rate of natural immunity of the human population have some effects on the $\mathbb{R}_0$ [20]. Izzati [21] formulated diphtheria epidemic and incorporated prevention and treatment as key factors that could curb the disease and examined the effects of vaccination on the transmission dynamics. Grasse [22] conducted a study on the effects of booster vaccines against tetanus and diphtheria. The results showed that booster vaccines against tetanus and diphtheria only provided long-lasting protection against tetanus. The level of protection was lower in people infected with diphtheria.

Diphtheria is a vaccine preventable disease. However, insufficient production of Diphtheria, Tetanus and Pertussis (DTP) vaccines by pharmaceutical industries was identified as one of the major causes of the prevalence of the disease. This was as a result of low demand and priority. The authors asserted that local, national and international efforts must be made to increase the production and availability of DTP vaccines [23]. Ilahi [24] formulated a model to determine the effectiveness of vaccines in the control of diphtheria in Indonesia. Findings from the research indicated that vaccines are very effective in reducing the spread and prevalence of diphtheria. Kanchanarat [25] formulated a mathematical model for predicting the optimal vaccine coverage level for the control of diphtheria. The mathematical model revealed the global dynamical features of the model. The results showed that the optimal level of vaccination required for the eradication of the disease should be less than the actual vaccination coverage. Fauzi [26] developed a model that incorporated DPT and booster vaccinations for the determination of $\mathbb{R}_0$. The authors suggested increasing the booster vaccination coverage rate by 15.90% as a possible approach of controlling diphtheria in West Java.

The proposed model distinguishes between exposed, asymptomatic, symptomatic and quarantined individuals, giving a more nuanced understanding of the disease dynamics. Additionally, the model incorporates bacteria concentration in the environment (B_c) as a dynamic component. The novelty lies in its detailed compartmental structure and the explicit representation effects of vaccination, the need for infected individuals to be quarantined and bacteria concentration in the environment, which together enhance its applicability and accuracy in assessing and managing diphtheria outbreaks.

2. Model Formulation

A deterministic dynamical model is proposed to study the transmission and control mechanisms of diphtheria. The human population is divided into seven mutually exclusive compartments - Susceptible $S(t)$, Vaccinated $V(t)$, Exposed $E(t)$, Asymptomatic $A(t)$, Symptomatic $I(t)$, Quarantined $Q(t)$ and Recovered $R(t)$. The concentration of bacteria in the environment is represented by $B_c(t)$. It is assumed that only symptomatic infected and quarantined individuals die due to the severity of diphtheria infection and that individuals in each of the classes of the model can die naturally.

Susceptible humans are those who may be exposed to diphtheria at the recruitment rate, α_h. This class is further populated due to loss of immunity by the recovered sub-class at the rate ω. This class is reduced due to the movement of people to the $V(t)$ compartment at the vaccine uptake rate, ν and $E(t)$ compartment at the rate, λ where

$$\lambda = \frac{\beta_h(\pi A(t) + I(t))}{N(t)} + \frac{\beta B_c(t)}{C + B_c(t)}, \tag{1}$$

represents the force of infection. β_h and β denote human to human transmissions rates for infected sub-classes $A(t)$, $I(t)$ and environment to human transmission rate for the bacteria concentration compartment $B_c(t)$ respectively. C is the carrying capacity of the environment. The vaccinated human compartment is formed at the vaccine uptake rate, ν. Since diptheria vaccines are not 100% efficacious [1], a fraction of the vaccinated humans become exposed to the disease at the rate, λ_v where $\lambda_v = (1-\varepsilon)\lambda$ and ϵ denotes vaccine efficacy. The exposed human compartment is populated at the rates λ and λ_v via the influx of people from the $S(t)$ and $V(t)$ compartments respectively. This class is depopulated because of the movement of people to the asymptomatic infected compartment at the rate, σ_1. The asymptomatic

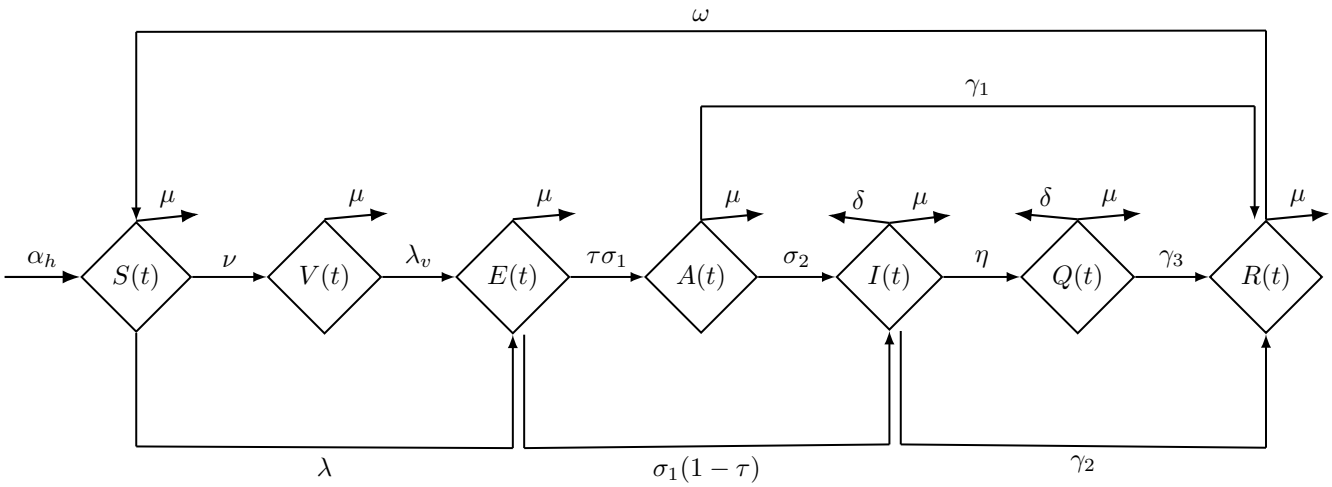

Figure 1. Flow Diagram of the system (2)

infected human compartment is generated at the rates, $\tau\sigma_1$. Individuals with latent infection progress to $I(t)$ compartment at a rate, σ_2 and recover at the rate, γ_l respectively. Individuals who are infected with diphtheria are generated at the rate, $\sigma_1(1-\tau)$ from $E(t)$ and σ_2 from $A(t)$ compartments respectively. This sub-class is reduced due to the movement of people to the $Q(t)$ and $R(t)$ compartments at the rates, η and γ_2 respectively. In order to reduce the rate at which infected humans spread diphtheria disease, there is a need to administer special medical care to the people in a quarantine [27–29]. In view of this, the quarantined human compartment is generated from the infected human population at the rate, η, and this sub-class is reduced at the rate, γ_3 due to the movement of people to the $R(t)$ compartment. People infected with diphtheria recover at the rates, γ_1, γ_2 and γ_3 from the $A(t), I(t)$ and $Q(t)$ sub-classes respectively. There is a reduction in the $R(t)$ compartment due to waning immunity at the rate ω.

The bacteria concentration compartment, $B_c(t)$, is generated at the rate, α_c where

$$\alpha_c = \alpha\left(1 - \frac{B_c(t)}{C}\right)B_c(t),$$

and α represents the growth rate of bacteria. This class is further populated at the rates ρ_1, ρ_2 and ρ_3 from the $A(t), I(t)$ and $Q(t)$ sub-classes respectively

The flow diagram for the proposed model's population dynamics is shown in Figure 1. The proposed model is given as:

$$\begin{aligned}
\frac{dS(t)}{dt} &= \alpha_h + \omega R(t) - \nu S(t) - \lambda S(t) - \mu S(t),\\
\frac{dV(t)}{dt} &= \nu S(t) - \lambda_v V(t) - \mu V(t),\\
\frac{dE(t)}{dt} &= \lambda S(t) + \lambda_v V(t) - \sigma_1 E(t) - \mu E(t),\\
\frac{dA(t)}{dt} &= \tau\sigma_1 E(t) - \sigma_2 A(t) - \gamma_1 A(t) - \mu A(t),\\
\frac{dI(t)}{dt} &= \sigma_1(1-\tau)E(t) + \sigma_2 A(t) - \eta I(t) - \gamma_2 I(t) - \delta I(t)\\
&\quad - \mu I(t),\\
\frac{dQ(t)}{dt} &= \eta I(t) - \gamma_3 Q(t) - \delta Q(t) - \mu Q(t),
\end{aligned} \tag{2}$$

$$\begin{aligned}
\frac{dR(t)}{dt} &= \gamma_1 A(t) + \gamma_2 I(t) + \gamma_3 Q(t) - \omega R(t) - \mu R(t),\\
\frac{dB_c(t)}{dt} &= \alpha_c + \rho_1 A(t) + \rho_2 I(t) + \rho_3 Q(t) - \mu_c B_c(t).
\end{aligned}$$

The parameters of the model are defined in Table 1 below

Table 1. Parameter description

Parameter	Description
α_h	Recruitment rate into the human population
α	The growth rate of bacteria
μ	Human natural death rate
μ_c	Bacteria natural death rate
π	Modification factor for $A(t)$ compartment
δ	Disease induced death
β_h	Human to human transmission rates for infected sub-compartments, $A(t)$ and $I(t)$
β	Environment to human transmission rate for the bacteria concentration compartment, $B_c(t)$
C	Carrying capacity of the environment
ω	Rate of loss of immunity by $R(t)$ compartment
ν	Vaccination rate for $S(t)$ compartment
τ	Proportion of exposed humans that progress to $A(t)$ compartment
$1-\tau$	Proportion of exposed humans that progress to $I(t)$ compartment
$\sigma_i, i = 1, 2$	Rate of infections of individuals in compartments $E(t)$ and $A(t)$
η	Rate of isolation for symptomatic infected individuals
$\gamma_i, i = 1, 2, 3$	Recovery rates of humans in compartments $A(t)$, $I(t)$ and $Q(t)$ respectively
$\rho_i, i = 1, 2, 3$	Shedding rate for $A(t)$, $I(t)$ and $Q(t)$ compartments

2.1. *The model analysis*

1. the invariant region
   The system (2) has a region defined by the set

$$\Omega(t) = \Big\{ (S(t) + V(t) + E(t) + A(t) + I(t) + Q(t) + R(t) + B_c(t)) \in \mathbb{R}^8_+ : N(t) < \frac{\alpha_h}{\mu_h} \Big\}.$$

   The following theorems demonstrate that system (2) is epidemiologically meaningful, prove its well-posedness

and establish that the model's solutions are uniformly bounded.

Theorem 1. *The region of the system (2) defined by the set $\Omega(t)$ is positively invariant with $\Omega(t) \geq 0 \in \mathbb{R}^8_+$*

Proof. The total population is defined as $N(t) = S(t) + V(t) + E(t) + A(t) + I(t) + Q(t) + R(t) + B_c(t)$. Thus,

$$\frac{dN(t)}{dt} = \frac{dS(t)}{dt} + \frac{dV(t)}{dt} + \frac{dE(t)}{dt} + \frac{dA(t)}{dt} + \frac{dI(t)}{dt} + \frac{dQ(t)}{dt} + \frac{dR(t)}{dt} + \frac{dB_c(t)}{dt}.$$

Hence,

$$\frac{dN(t)}{dt} \leq \alpha_h - \mu N(t),$$
$$(\alpha_h - \mu N(t)) \geq (Ae^{-\mu t}),$$

where A is a constant of integration. Let $N(0) = N_0$. Then,

$$(\alpha_h - \mu N_0) \geq A,$$
$$N(t) \leq \frac{\alpha_h}{\mu} - \frac{(\alpha_h - \mu N_0)}{\mu} e^{-\mu t}.$$

Thus, $N(t) \in [0, \frac{\alpha_h}{\mu}]$. Hence, the invariant region containing the solutions to the system (2) is given by

$$\Omega = [(S(t), V(t), E(t), A(t), I(t), Q(t), R(t), B_c(t)) \in R^8_+ : N(t) \leq \frac{\alpha_h}{\mu}].$$

This implies that the system (2) is biologically and mathematically well-posed and that the region which contains the solutions to the model equations is positively invariant. □

2.2. The positivity theorem

Theorem 2. *Given that the initial conditions of system (2) are $S_0 > 0, V_0 > 0, E_0 > 0, A_0 > 0, I_0 > 0, Q_0 > 0, \mathbb{R}_0 > 0, B_{c0} > 0$. There exists $\Omega = S(t), V(t), E(t), A(t), I(t), Q(t), R(t), B_c(t) \in R^8_+ : S_0 > 0, V_0 > 0, E_0 > 0, A_0 > 0, I_0 > 0, Q_0 > 0, \mathbb{R}_0 > 0, B_{c0} > 0$: $(0, \text{inf}) \longrightarrow (0, \text{inf})$ which solves system (2).*

Proof. Assume that $\hat{t} = \sup\{S(0) > 0, V(0) > 0, E(0) > 0, A(0) > 0, I(0) > 0, Q(0) > 0, R(0) > 0, B_c(0) > 0\}$, this implies that $\hat{t} > 0$. Hence,

$$\frac{dS(t)}{dt} \geq -\left((\nu + \mu) + \frac{\beta_h(\pi A(t) + I(t))}{N(t)} + \frac{\beta B_c(t)}{C + B_c(t)}\right) S_h.$$

Using the method of separation of variables, we have

$$\frac{dS(t)}{S(t)} \geq -\left((\nu + \mu) + \frac{\beta_h(\pi A(t) + I(t))}{N(t)} + \frac{\beta B_c(t)}{C + B_c(t)}\right) dt.$$

Integrating, we get

$$S(t) \geq S(0)e^{-\left((\nu+\mu)t + \int_0^t \tilde{\varphi}(\eta)d\eta\right)} \geq 0, \quad \forall\, t \geq 0.$$

where $\tilde{\varphi}(\eta) = \frac{\beta_h(\pi A(t)+I(t))}{N(t)} + \frac{\beta B_c(t)}{C+B_c(t)}$.
Similarly,

$$\begin{aligned}
V(t) &\geq V(0)e^{-\left(\mu t + (1-\varepsilon)\int_0^t \tilde{\varphi}(\eta)d\eta\right)t} \geq 0, && \forall\, t \geq 0,\\
E(t) &\geq E(0)e^{-(\sigma_1+\mu)t} \geq 0, && \forall\, t \geq 0,\\
A(t) &\geq A(0)e^{-(\sigma_2+\gamma_1+\mu)t} \geq 0, && \forall\, t \geq 0,\\
I(t) &\geq I(0)e^{-(\eta+\gamma_2+\delta+\mu)t} \geq 0, && \forall\, t \geq 0,\\
Q(t) &\geq Q(0)e^{-(\gamma_3+\delta+\mu)t} \geq 0, && \forall\, t \geq 0,\\
R(t) &\geq R(0)e^{-(\omega+\mu)t} \geq 0, && \forall\, t \geq 0,\\
B_c(t) &\geq B_c(0)e^{-\mu_c t} \geq 0, && \forall\, t \geq 0.
\end{aligned}$$

□

2.3. The positivity theorem

1. the disease free equilibrium point (DFE):
There is non-existence of infections or recovery at the DFE. Hence, at the DFE, the infected human is zero i.e. $E(t) = A(t) = I(t) = Q(t) = R(t) = 0$. Thus, the DFE is obtained as

$$\mathcal{E}^0 = \left(S^0 = \frac{\alpha_h}{\nu + \mu},\ V^0 = \frac{\nu\alpha_h}{\mu(\nu + \mu)},\ E^0 = 0,\ A^0 = 0,\ I^0 = 0,\ Q^0 = 0,\ R^0 = 0,\ B_c^0 = \frac{\alpha_c}{\mu_c}\right). \tag{3}$$

2. the basic reproduction number
The basic reproduction number, $\mathbb{R}_0$, for system (2) is given by the spectral radius of the next-generation matrix, FV^{-1}. This implies that

$$F = \begin{pmatrix} 0 & \frac{\beta_h \pi D^0}{N^0} & \frac{\beta_h D^0}{N^0} & 0 & \frac{\beta D^0}{C} \\ 0 & 0 & 0 & 0 & 0 \\ 0 & 0 & 0 & 0 & 0 \\ 0 & 0 & 0 & 0 & 0 \\ 0 & 0 & 0 & 0 & 0 \end{pmatrix} \tag{4}$$

where $D^0 = S^0 + (1 - \varepsilon)V^0$ and $N^0 = \frac{\alpha_h}{\nu+\mu}$.

$$V = \begin{pmatrix} k_3 & 0 & 0 & 0 & 0 \\ -\tau\,\sigma_1 & k_4 & 0 & 0 & 0 \\ \sigma_1\,(1-\tau) & -\sigma_2 & k_5 & 0 & 0 \\ 0 & 0 & -\eta & k_6 & 0 \\ 0 & -\rho_1 & -\rho_2 & -\rho_3 & k_8 \end{pmatrix} \tag{5}$$

where $k_3 = \sigma_1 + \mu$, $k_4 = \sigma_2 + \gamma_1 + \mu$, $k_5 = \eta + \gamma_2 + \delta + \mu$, $k_6 = \gamma_3 + \delta + \mu$, $k_7 = \omega + \mu$ and $k_8 = \mu_c - \alpha_c$. Thus, $\mathbb{R}_0$ is expressed as:

$$\begin{aligned}
\mathbb{R}_0 &= \frac{\alpha_h\big(\tau a_1 + a_2 k_4\big)k_6 + \beta\eta\rho_3 a_3 N\big)\big(\mu - k_3\big)}{k_3 k_4 k_5 k_6 k_8 C N(\nu + \mu)},\\
a_1 &= \beta\big(2\rho_2 k_4 + \big(\gamma_1 + \mu\big)\rho_2 + \rho_1 k_5\big)N + \beta_h k_8 C\big(\gamma_1 + \mu - \pi k_5 - 2k_4\big),\\
a_2 &= \beta_h k_8 C + \beta\rho_2 N,\\
a_3 &= \big(\gamma_1 + \mu - 2k_4\big)\tau + k_4,
\end{aligned} \tag{6}$$

Thus, diphtheria can be eradicated from the population if $\mathbb{R}_0 < 1$ according to the following theorem:

Theorem 3. *The disease-free equilibrium, $\mathcal{E}^0$, of the system (2) and given by eq. (3), is locally asymptotically stable (LAS) when $\mathbb{R}_0 < 1$, and unstable when $\mathbb{R}_0 > 1$.*

Proof. In order to prove Theorem 3, the method outlined in [30, 31] is adopted. We begin by deriving the Jacobian matrix of system (2) at the $\mathcal{E}^0$. The Jacobian matrix is expressed as:

$$J(\mathcal{E}^0) = \begin{pmatrix} J_1 & 0 & 0 & J_2 & J_3 & 0 & \omega & J_3 \\ \nu & -\mu & 0 & 0 & 0 & 0 & 0 & 0 \\ 0 & 0 & J_4 & J_5 & J_6 & 0 & 0 & J_6 \\ 0 & 0 & \tau\sigma_1 & J_7 & 0 & 0 & 0 & 0 \\ 0 & 0 & J_8 & \sigma_2 & J_9 & 0 & 0 & 0 \\ 0 & 0 & 0 & 0 & \eta & J_{10} & 0 & 0 \\ 0 & 0 & 0 & \gamma_1 & \gamma_2 & \gamma_3 & J_{11} & 0 \\ 0 & 0 & 0 & \rho_1 & \rho_2 & \rho_3 & 0 & -\mu_c \end{pmatrix},$$

$$\begin{aligned} J_1 &= -\nu-\mu, & J_2 &= -\frac{\beta_h\pi\alpha_h}{N(\nu+\mu)}, \\ J_3 &= -\frac{\beta_h\alpha_h}{N(\nu+\mu)}, & J_4 &= -\sigma_1-\mu, \\ J_5 &= \frac{\beta_h\pi\alpha_h}{N(\nu+\mu)}, & J_6 &= \frac{\beta_h\alpha_h}{N(\nu+\mu)}, \\ J_7 &= -\mu-\gamma_1-\sigma_2, & J_8 &= \sigma_1(1-\tau), \\ J_9 &= -\eta-\gamma_2-\delta-\mu, & J_{10} &= -\delta-\gamma-\mu, \\ J_{11} &= -\mu-\omega, \end{aligned} \tag{7}$$

The characteristic polynomial, $P(\lambda^*)$, corresponding to eq. (7) can be expressed as:

$$P(\lambda^*) = |J(\mathcal{E}^0) - \lambda^*\mathbb{I}_8|,$$

$$P(\lambda^*) = \begin{vmatrix} P_{11} & 0 & 0 & J_2 & J_3 & 0 & \omega & J_3 \\ \nu & P_{22} & 0 & 0 & 0 & 0 & 0 & 0 \\ 0 & 0 & P_{33} & J_5 & J_6 & 0 & 0 & J_6 \\ 0 & 0 & \tau\sigma_1 & P_{44} & 0 & 0 & 0 & 0 \\ 0 & 0 & J_8 & \sigma_2 & P_{55} & 0 & 0 & 0 \\ 0 & 0 & 0 & 0 & \eta & P_{66} & 0 & 0 \\ 0 & 0 & 0 & \gamma_1 & \gamma_2 & \gamma_3 & P_{77} & 0 \\ 0 & 0 & 0 & \rho_1 & \rho_2 & \rho_3 & 0 & P_{88} \end{vmatrix},$$

$$\begin{aligned} P_{11} &= -\nu-\mu-\lambda^*, \\ P_{22} &= -\mu-\lambda^*, \\ P_{33} &= -\sigma_1-\mu-\lambda^*, \\ P_{44} &= -\mu-\gamma_1-\sigma_2-\lambda^*, \\ P_{55} &= -\eta-\gamma_2-\delta-\mu-\lambda^*, \\ P_{66} &= -\delta-\gamma-\mu-\lambda^*, \\ P_{77} &= -\mu-\omega-\lambda^*, \\ P_{88} &= -\mu_c-\lambda^*. \end{aligned} \tag{8}$$

Therefore, the first three eigenvalues corresponding to eq. (8) are given by:

$$\lambda_i^* = \begin{pmatrix} -\nu-\mu \\ -\mu \\ -\mu-\omega \end{pmatrix} \tag{9}$$

The remaining eigenvalues are derived from the sub-matrix corresponding to the reduced system:

$$\mathcal{J} = \begin{pmatrix} J_4 & J_5 & J_6 & 0 & J_6 \\ \tau\sigma_1 & J_7 & 0 & 0 & 0 \\ J_8 & \sigma_2 & J_9 & 0 & 0 \\ 0 & 0 & \eta & J_{10} & 0 \\ 0 & \rho_1 & \rho_2 & \rho_3 & -\mu_c \end{pmatrix}, \tag{10}$$

Additionally, based on the Routh-Hurwitz criterion, the matrix $\mathcal{J}$ will possess all real and negative eigenvalues if $Tr(\mathcal{J}) < 0$ and $Det(\mathcal{J}) > 0$.
From eq. (10),

$$\begin{aligned} Tr(\mathcal{J}) =& -\sigma_1 - 4\mu - \gamma_1 - \sigma_2 - \eta - \gamma_2 - 2\delta - \gamma_3 - \mu_c < 0, \\ Det(\mathcal{J}) =& \frac{1}{NC(\nu+\mu)}\big((\beta((\rho_2-\rho_3)\mu + (k_5-\gamma_2-\delta)\rho_3 + \rho_2(\gamma_3 \\ &+\delta))N + \beta_h(\delta+\mu+\gamma_3)\mu_c C)\alpha_h k_4\sigma_1(1-\tau) - (\mu \\ &- k_3)(\beta((-\rho_2+\rho_3)\mu^2 + ((\rho_2-\rho_3)k_4 + (-k_5+\gamma_1 \\ &+\gamma_2+\delta)\rho_3 - \rho_2\delta + k_5\rho_1 - \rho_2(\gamma_1+\gamma_3))\mu + ((k_5-\gamma_2 \\ &-\delta)\rho_3 + \rho_2(\gamma_3+\delta))k_4 - \gamma_1(k_5-\gamma_2-\delta)\rho_3 + (\gamma_3 \\ &+\delta)(-\gamma_1\rho_2 + k_5\rho_1))N + C\mu_c\beta_h(\delta+\mu+\gamma_3)(\pi k_5 - \mu \\ &- \gamma_1 + k_4))\tau\alpha_h - k_3k_4k_5(\nu+\mu)(\delta+\mu+\gamma_3)\mu_c NC) \end{aligned}$$

The determinant above can be rewritten as

$$\frac{k_3(b_1-b_2-b_3)k_4k_6k_5k_8}{b_4-b_5}(1-\mathbb{R}_0) > 0 \text{ if } \mathbb{R}_0 < 1,$$

where

$$\begin{aligned} b_1 &= k_3k_4k_5(\nu+\mu)(\delta+\mu+\gamma_3)\mu_c NC, \\ b_2 &= \alpha_h A_1 k_4\sigma_1(1-\tau), \\ b_3 &= \alpha_h A_2\tau(k_3-\mu), \\ b_4 &= A_3(k_3-\mu)\alpha_h, \\ b_5 &= k_3k_4k_5k_6k_8(\nu+\mu)CN, \\ A_1 &= ((\rho_2-\rho_3)\mu + (k_5-\gamma_2-\delta)\rho_3 + \rho_2(\delta+\gamma_3))\beta N \\ &\quad + \beta_h(\delta+\mu+\gamma_3)\mu_c C, \\ A_2 &= ((-\rho_2+\rho_3)\mu^2 + ((\rho_2-\rho_3)k_4 + (-k_5+\gamma_1 \\ &\quad +\gamma_2+\delta)\rho_3 + (-\delta-\gamma_1-\gamma_3)\rho_2 + k_5\rho_1)\mu + ((k_5 \\ &\quad -\gamma_2-\delta)\rho_3 + \rho_2(\delta+\gamma_3))k_4 + \gamma_1(-k_5+\gamma_2 \\ &\quad +\delta)\rho_3 + (\delta+\gamma_3)(-\gamma_1\rho_2 + k_5\rho_1))\beta N \\ &\quad + C\mu_c\beta_h(\delta+\mu+\gamma_3)(\pi k_5 - \mu - \gamma_1 + k_4), \\ A_3 &= (((k_6\rho_2+\rho_3\eta)\mu - 2(\rho_3\eta + k_6\rho_2)k_4 + \rho_3\gamma_1\eta \\ &\quad + k_6(k_5\rho_1 - \gamma_1\rho_2))\beta N + Ck_6k_8\beta_h(\gamma_1 + \\ &\quad \mu - k_5\pi - 2k_4))\tau + k_4(\beta(\rho_3\eta + k_6\rho_2)N \\ &\quad + Ck_6k_8\beta_h). \end{aligned}$$

If $\mathbb{R}_0 < 1$, both eigenvalues of the matrix (10) will be real and negative, indicating that the $\mathcal{E}^0$ is LAS. Conversely, when $\mathbb{R}_0 > 1$, the eigenvalues become unstable, leading to the instability of $\mathcal{E}^0$. Additionally, by the Poincaré-Lyapunov theorem, since the eigenvalues of $J(\mathcal{E}^0)$ have negative real parts, as shown in eq. (9), $\mathcal{E}^0$ is indeed LAS. □

3. the endemic equilibrium point (EEP)
At the EEP, infections persist in the population, and all state variables of system (2) are considered non-negative. For instance, if I^{**} is non-negative in the system (2), then there exists a unique endemic equilibrium point for the system. This occurs when $\mathbb{R}_0 > 1$. Hence, the EEP is defined as

$$\mathcal{E}^1 = (S^{**}(t), V^{**}(t), E^{**}(t), A^{**}(t), I^{**}(t), Q^{**}(t), R^{**}(t), B_c^{**}(t)) \in R_+^8,$$

and it satisfies the following conditions:

$$\frac{dN(t)}{dt} = \frac{dS(t)}{dt} + \frac{dV(t)}{dt} + \frac{dE(t)}{dt} + \frac{dA(t)}{dt} + \frac{dI(t)}{dt} + \frac{dQ(t)}{dt} + \frac{dR(t)}{dt} + \frac{dB_c(t)}{dt}.$$

Due to the complexity of system (2), each state variable is expressed in terms of the steady state of I^{**}. Accordingly,

$$\begin{aligned}
S^{**} &= \frac{c_1\tau + c_2k_4}{c_3k_6k_7} I^{**},\\
V^{**} &= \frac{\nu\,(c_1\tau + c_2k_4)}{c_3k_6k_7\,((1-\epsilon)\,\lambda^{**} + \mu)} I^{**},\\
E^{**} &= \frac{\lambda^{**}\,((1-\epsilon)\,\lambda^{**} - \nu\epsilon + \mu + \nu)\,c_4}{c_5k_3k_6k_7} I^{**},\\
A^{**} &= \frac{k_5\tau}{\sigma_2\tau + k_4 - k_4\tau} I^{**},\\
Q^{**} &= \frac{\eta}{k_6} I^{**},\\
R^{**} &= \frac{c_6\tau + k_4\,(\eta\gamma_3 + \gamma_2k_6)}{k_7\,((\sigma_2 - k_4)\,\tau + k_4)\,k_6} I^{**},\\
B_c^{**} &= \frac{c_7\tau + ((\alpha_c + \rho_2)\,k_6 + \eta\rho_3)\,k_4}{((\sigma_2 - k_4)\,\tau + k_4)\,\mu_ck_6} I^{**},\\
c_1 &= ((-\omega\gamma_2 - \alpha_hk_7)\,k_6 - \eta\gamma_3\omega)\,k_4 + \big((\gamma_1k_5 + \gamma_2\sigma_2)\omega + \alpha_h\sigma_2k_7\big)k_6 + \eta\gamma_3\sigma_2\omega,\\
c_2 &= (\omega\gamma_2 + \alpha_hk_7)\,k_6 + \eta\gamma_3\omega,\\
c_3 &= (\lambda^{**} + k_1)\,((\sigma_2 - k_4)\,\tau + k_4),\\
c_4 &= \big(c_2k_4 + ((-\gamma_1k_5 - \gamma_2\sigma_2)\,\omega - \alpha_h\sigma_2k_7)\,k_6 - \eta\gamma_3\sigma_2\omega\big)\tau - c_2k_4,\\
c_5 &= ((1-\epsilon)\,\lambda^{**} + \mu)\,(\lambda^{**} + k_1)\,((k_4 - \sigma_2)\,\tau - k_4),\\
c_6 &= (-\eta\gamma_3 - \gamma_2k_6)\,k_4 + (\gamma_1k_5 + \gamma_2\sigma_2)\,k_6 + \eta\sigma_2\gamma_3,\\
c_7 &= ((-\alpha_c - \rho_2)\,k_6 - \eta\rho_3)\,k_4 + ((\alpha_c + \rho_2)\,\sigma_2 + k_5\rho_1)k_6 + \eta\sigma_2\rho_3,
\end{aligned} \tag{11}$$

where $I^{**} = \frac{\tau\,\sigma_2 + k_4 - \tau\,k_4}{\tau\,k_5} A^*$ and the force of infection is given by $\lambda^{**} = \frac{\beta_h(\pi A^{**}(t) + I^{**}(t))}{N^{**}(t)} + \frac{\beta B_c^{**}(t)}{C + B_c^{**}(t)}$.

Theorem 4. *The $\mathcal{E}^1$ will be GAS as long as $\mathbb{R}_0 > 1$.*

Proof. The Lyapunov-Lasalle Invariance Principle, which requires the analysis of a Lyapunov candidate function for the equilibrium point, $\mathcal{E}_1$, is used to prove the theorem. let $\mathcal{V}$ be a continuously differentiable, scalar function (Lyapunov function) defined as

$$\mathcal{V} = \sum_{\mathcal{X}} (\mathcal{X} - \mathcal{X}^{**}) \tag{12}$$

where $\mathcal{X} = S(t), V(t), E(t), A(t), I(t), Q(t), R(t), B_c(t)$. This implies that

$$\begin{aligned}
\mathcal{V} = &\frac{1}{2}\big(S - S^{**}\big)^2 + \frac{1}{2}\big(V - V^{**}\big)^2 + \frac{1}{2}\big(E - E^{**}\big)^2\\
&+ \frac{1}{2}\big(A - A^{**}\big)^2 + \frac{1}{2}\big(I - I^{**}\big)^2 + \frac{1}{2}\big(Q - Q^{**}\big)^2\\
&+ \frac{1}{2}\big(R - R^{**}\big)^2 + \frac{1}{2}\big(B_c - B_c^{**}\big)^2.
\end{aligned} \tag{13}$$

By differentiating eq. (13), we obtain

$$\begin{aligned}
\dot{\mathcal{V}} = &\big(S - S^{**}\big)\dot{S} + \big(V - V^{**}\big)\dot{V} + \big(E - E^{**}\big)\dot{E} + \big(A\\
&- A^{**}\big)\dot{A} + \big(I - I^{**}\big)\dot{I} + \big(Q - Q^{**}\big)\dot{Q} + \big(R\\
&- R^{**}\big)\dot{R} + \big(B_c - B_c^{**}\big)\dot{B}_c,\\
= &\Big(\big(\alpha_h + \omega R\big)S + \big(\nu + \lambda + \mu\big)S^{**}S + \nu SV + \big(\lambda_v\\
&+ \mu\big)V^{**}V + \lambda SE + \lambda_vVE + \big(\sigma_1 + \mu\big)E^{**}E\\
&+ \tau\sigma_1EA + (\sigma_2 + \gamma_1 + \mu)A^{**}A + \sigma_1(1-\tau)EI\\
&+ \sigma_2AI + \big(\eta + \gamma_2 + \delta + \mu\big)I^{**}I + \eta IQ + (\gamma_3 + \delta\\
&+ \mu)Q^{**}Q + \gamma_1AR + \gamma_2IR + \gamma_3QR + (\omega + \mu)R^{**}R\\
&+ \alpha_cB_c + \rho_1AB_c + \rho_2IB_c + \rho_3QB_c + \mu_cB_c^{**}B_c\Big)\\
&- \Big(\big(\nu + \lambda + \mu\big)S + \big(\alpha_h + \omega R\big)S^{**}S + \big(\lambda_v + \mu\big)V\\
&+ \nu SV^{**}V + \big(\sigma_1 + \mu\big)E + \lambda SE^{**}E + \lambda_vVE^{**}E\\
&+ (\sigma_2 + \gamma_1 + \mu)A + \tau\sigma_1EA^{**}A + \big(\eta + \gamma_2 + \delta + \mu\big)I\\
&+ \sigma_1(1-\tau)EI^{**}I + \sigma_2AI^{**}I + (\gamma_3 + \delta + \mu)Q\\
&+ \eta IQ^{**}Q + (\omega + \mu)R + \gamma_1AR^{**}R + \gamma_2IR^{**}R\\
&+ \gamma_3QR^{**}R + \mu_cB_c + \alpha_cB_c^{**}B_c + \rho_1AB_c^{**}B_c\\
&+ \rho_2IB_c^{**}B_c + \rho_3QB_c^{**}B_c\Big)
\end{aligned} \tag{14}$$

Note that

$$\begin{aligned}
&(\dot{S} - \dot{S}^{**}) + (\dot{V} - \dot{V}^{**}) + (\dot{E} - \dot{E}^{**}) + (\dot{A} - \dot{A}^{**})\\
&+(\dot{I} - \dot{I}^{**}) + (\dot{Q} - \dot{Q}^{**}) + (\dot{R} - \dot{R}^{**}) + (\dot{B}_c - \dot{B}_c{}^{**})\\
&=\\
&-(\nu + \lambda + \mu)(S - S^{**})^2 - (\lambda_v + \mu)(V - V^{**})^2 - (\sigma_1\\
&+\mu)(E - E^{**})^2 - (\sigma_2 + \gamma_1 + \mu)(A - A^{**})^2 -\\
&(\eta + \gamma_2 + \delta + \mu)(I - I^{**})^2 - (\gamma_3 + \delta + \mu)(Q - Q^{**})^2 - (\omega\\
&+\mu)(R - R^{**})^2 - \mu_c(B_c - B_c^{**})^2
\end{aligned} \tag{15}$$

These are all negative or zero. At the endemic equilibrium, all derivatives $\dot{\mathcal{X}}^{**} = 0$. Hence, $\dot{\mathcal{V}} = 0$ iff $\mathcal{X} = \dot{\mathcal{X}}^{**}$. For other points, since all the diagonal terms are of the form $(\mathcal{X} - \mathcal{X}^{**})^2$, this implies that $\dot{\mathcal{V}} \leq 0$. Hence, $\dot{\mathcal{V}}$ is negative semidefinite and zero only at the endemic equilibrium. As a result, the largest compact invariant set within $\left\{\left(S, V, E, A, I, Q, R, B_c\right) \in \Omega : \mathcal{V} \leq 0\right\}$ is the $\mathcal{E}^1$. Thus, by applying the Lyapunov-LaSalle Invariance Principle, it follows that as $t \to \infty$, all solutions within the set Ω will converge to $\mathcal{E}^1$ when $\mathbb{R}_0 > 1$. Therefore, the $\mathcal{E}^1$ is GAS. Notably,

the epidemiological significance of this finding is that diphtheria will persist and spread within the population for as long as $\mathbb{R}_0 > 1$. □

2.4. Parameter Value Estimation

The recruitment rate into the human compartment (α_h): The Susceptible Human Population is populated at the rate, α_h. The average recruitment per unit time into the susceptible human population is estimated from the annual population growth of Nigeria between the year 2013 to 2023. The average annual population increase of Nigeria within this period is 2.50 million per year [32, 33]. Thus, the recruitment rate per day is given as $\alpha_h = \frac{2.50}{365} = 0.0069$ per day.

Natural death rate (μ_h): In Nigeria, life expectancy at birth in 2023 was about 61.79 years [34]. Hence, $\mu = \frac{1}{61.79\times 365} = 0.00004434$ per day.

Disease-induced death rate (δ_h): The mortality rate due to diphtheria is estimated as $\delta = \frac{828}{27991} = 0.0296$ per day [1].

The recovery rate for exposed human population can be taken as $\gamma_1 = \frac{1}{14}$ per day [14]. A patient needs to rest for at least four weeks after the anti-toxin antibiotics has taken effect for full recovery [35]. Hence, $\gamma_2 = \gamma_3 = \frac{1}{28}$ per day.

From the concept of half life [36], the rate of progression from exposed to asymptomatic infected compartment (σ_1) is estimated based on the fact that $0 - 26\%$ of individuals infected with diphtheria do not show any symptom of the disease [37]. The incubation period of diphtheria has a maximum value of 10 days [38]. Hence, $\tau = 0.26$. Furthermore, $\sigma_1 = -\frac{1}{10}ln(0.77) = 0.0261$ per day. It is assumed that asymptomatic infected are twice likely to transmit diphtheria when compared to people in the exposed human compartments. Hence, $\sigma_2 = 2 \times 0.0261 = 0.0522$ per day.

Others are $\beta_h = 0.0357$ per day [14], $\beta = \frac{1}{28}$ (Assumed), $\mu_c = 0.0345$ per day [25], $\rho_1 = 0.9$ per day [25], $\rho_2 = 0.8$ per day [25], $\rho_3 = 0.7$ per day (Assumed), $\pi = 0.5$ [14], $\omega = 0.0667$ per day(Assumed), $C = 500,000$ [14], and $\varepsilon = 0.85$ [14], $\alpha = 0.014$ per day [14].

2.5. Sensitivity Analysis

The sensitivity index (SI) of all the model parameters of system (2) is obtained by calculating the normalized forward SI for each parameter of $\mathbb{R}_0$ with respect to a parameter Ψ [39–44]. Hence, the effects of small changes in parameter values with positive and negative SI on $\mathbb{R}_0$ are examined.

Definition 1. The normalized forward SI of $\mathbb{R}_0$, with respect to a parameter Ψ, is defined by

$$S_{\Psi}^{\mathbb{R}_0} = \frac{\partial \mathbb{R}_0}{\partial \Psi} \times \frac{\Psi}{\mathbb{R}_0} \tag{16}$$

Equation 16 is used to obtain the expression for the SI of each of the parameters of $\mathbb{R}_0$. For example, the SI of $\mathbb{R}_0$ with respect to π can be written as

$$S_{\pi}^{\mathbb{R}_0} = \frac{\partial \mathbb{R}_0}{\partial \pi} \times \frac{\pi}{\mathbb{R}_0} \approx \frac{11}{100}$$

Therefore, the SI of each of the parameter of $\mathbb{R}_0$ can be derived from equation 16. Thus, the SI of each parameter with respect to $\mathbb{R}_0$ evaluated using the parameter values in subsection: 2.4.

Table 2 indicates that the sign of the SI of the following parameters $\pi, \alpha, \beta, \nu, \beta_h, \rho_1, \rho_2, \rho_3, \sigma_1, \sigma_2$ is positive while it is negative for $C, \delta, \eta, \mu, \tau, \alpha_h, \gamma_1, \gamma_2, \gamma_3, \mu_c$. The positive SI sign of the diphtheria model indicates that any increase or decrease in these parameters will lead to a corresponding rise or fall in the threshold for diphtheria disease. On the other hand, while the positive SI values signify a direct proportionality between the parameters and the resulting value of $\mathbb{R}_0$, the negative SI values indicate an inverse relationship. Thus, an increase in the value of any parameter with a negative SI will lead to a decrease in $\mathbb{R}_0$, and vice-versa. For instance, $S_{\pi}^{\mathbb{R}_0} = +11$ means that a 100% increase in the value of π will lead to an 11% increase of in the value of the basic reproduction. Similarly, $S_{\eta}^{\mathbb{R}_0} \approx -30$ means that a 100% increase in the value of η will decrease $\mathbb{R}_0$ by 30%. In view of the sensitivity indices in Table 2, control measures that will reduce the values of the parameters with positive SI and increase the values of the parameters with negative SI should be employed in order to effectively curtail the transmission and spread of diphtheria infection.

Table 2. SI of $\mathbb{R}_0$ with respect to each of the parameters of model

Parameter	Sign of SI	Value
π	+ve	0.1075942254
α	+ve	0.02171276480
β	+ve	0.03179369146
ν	+ve	0.9679917050
β_h	+ve	0.9682063088
ρ_1	+ve	0.005083408703
ρ_2	+ve	0.01807136619
ρ_3	+ve	0.008638916567
σ_1	+ve	0.001695969292
σ_2	+ve	0.01865842862
C	-ve	0.03179369076
δ	-ve	0.2638461360
η	-ve	0.3048611609
μ	-ve	0.001958110176
τ	-ve	0.04419557653
α_h	-ve	0.9682063090
γ_1	-ve	0.1312545527
γ_2	-ve	0.3135000775
γ_3	-ve	0.004719755211
μ_c	-ve	0.05350645610

3. Formulation of an Optimal Control Problem (OCP)

The system of diphtheria dynamics given in system (2) is extended into an OCP by introducing four time-dependent variables $\psi_i(t), i = 1, 2, 3, 4$ where:

(i) $\psi_1(t)$ = personal protection;
(ii) $\psi_2(t)$ = booster vaccine administration;
(iii) $\psi_3(t)$ = detection/treatment of the asymptomatic infected humans; and
(iv) $\psi_4(t)$ = reduction of bacteria concentration.

The description of each of the four control variables is given below:

(i) The control variable $0 \leq \psi_1(t) \leq 1$ represents personal protection such as avoiding contact with individuals that

have symptoms of diphtheria. Other measures are frequent hand washing with soap and water, the use of nose masks or covering one's mouth and nose with tissue especially when coughing. Hence, the probability of diphtheria bacteria transmission from infected humans or surface to susceptible individuals due to $\psi_1(t)$ becomes $P^c_\lambda = (1-\psi_1(t))\lambda S(t)$.

(ii) The control variable $0 \leq \psi_2(t) \leq 1$ denotes booster vaccines and it is introduced because diphtheria vaccines fade with time. Infants who received all the doses of recommended diptheria vaccines before the age of seven are expected to get their first diphtheria booster vaccine at about age seven or twelve. Thereafter, it is recommended that the booster vaccines will be administered at 10-year intervals [45–47]. Thus, the probability of the effects of diphtheria booster vaccines on the bacteria transmission from vaccinated humans to exposed humans in view of $\psi_2(t)$ is given as $P^c_{\nu_1} = \psi_2(t)\nu_1 V(t)$.

(iii) The control variable $0 \leq \psi_3(t) \leq 1$ stands for the preventive strategies employed to detect and treat asymptomatic infected humans. The control involves screening of susceptible individuals for early detection of humans who have been exposed to the disease [16, 45, 48, 49]. Therefore, the probability of the progression of individuals from exposed humans to asymptomatic and infectious humans in the presence of $\psi_3(t)$ are $P^c_{\sigma_{1A}} = \tau\psi_3(t)\sigma_1 E(t)$ and $P^c_{\sigma_{1I}} = (1-\tau)\psi_3(t)\sigma_1 E(t)$ respectively.

(iv) The control variable $0 \leq \psi_4(t) \leq 1$ include all efforts by medical personnel and health authorities to reduce diphtheria bacteria concentration. In addition, diphtheria antitoxin prevents the bacteria toxin from multiplying and damaging the body of an infected person. In view of this, the probability of reducing diphtheria bacteria concentration in asymptomatic infected, symptomatic infected and quarantined humans based on $\psi_4(t)$ are given by $P^c_{\rho_1} = (1-\psi_4(t))\rho_1 A(t)$, $P^c_{\rho_2} = (1-\psi_4(t))\rho_2 I(t)$ and $P^c_{\rho_3} = (1-\psi_4(t))\rho_3 Q(t)$ respectively [16, 45, 46].

Our aim is to minimize the following cost functional

$$J(\psi_1,\psi_2,\psi_3,\psi_4) = \int_0^{t_f} (\kappa_1 A(t) + \kappa_2 I(t) + \kappa_3 Q(t) + \kappa_4 B_c(t)) + \frac{1}{2}\sum_{i=1}^{4}\omega_i\psi_i^2(t))dt, \quad (17)$$

subject to the non-linear ordinary differential equations below:

$$\begin{aligned}
\frac{dS(t)}{dt} &= \alpha_h + \omega R(t) - \nu S(t) - (1-\psi_1(t))\lambda S(t) - \mu S(t),\\
\frac{dV(t)}{dt} &= \nu S(t) - \psi_2(t)\lambda_v V(t) - \mu V(t),\\
\frac{dE(t)}{dt} &= (1-\psi_1(t))\lambda S(t) + \psi_2(t)\lambda_v V(t) - \sigma_1 E(t) - \mu E(t),\\
\frac{dA(t)}{dt} &= \tau(t)\sigma_1 E(t) - \psi_3(t)\sigma_2 A(t) - \gamma_1 A(t) - \mu A(t),\\
\frac{dI(t)}{dt} &= (1-\tau)\sigma_1 E(t) + \psi_3(t)\sigma_2 A(t) - \eta I(t) - \gamma_2 I(t) - \delta I(t) - \mu I(t),\\
\frac{dQ(t)}{dt} &= \eta I(t) - \gamma_3 Q(t) - \delta Q(t) - \mu Q(t),\\
\frac{dR(t)}{dt} &= \gamma_1 A(t) + \gamma_2 I(t) + \gamma_3 Q(t) - \omega R(t) - \mu R(t),\\
\frac{dB_c(t)}{dt} &= \alpha_c + (1-\psi_4(t))(\rho_1 A(t) + \rho_2 I(t) + \rho_3 Q(t)) - \mu_c B_c(t),
\end{aligned} \quad (18)$$

where t_f stands for the maximum or final time for the implementation of the control strategies and the balancing weight constants, $\kappa_i > 0$, $i = 1,2,3,4$, are for asymptomatic individuals, symptomatic individuals, Quarantined individuals and bacteria concentration respectively. The terms $\frac{1}{2}\omega_i\psi_i^2(t)$, $i = 1,2,3,4$ represent the costs of implementing personal protection, administration of booster vaccines, early detection and treatment of asymptomatic infected individuals and reduction of diphtheria bacteria concentration in the environment respectively.

By adopting the concept in [50–53], we seek to minimize the objective functional by finding the optimal controls $\psi_1^*(t)$, $\psi_2^*(t), \psi_3^*(t), \psi_4^*(t)$ such that

$$J(\psi_1^*(t),\psi_2^*(t),\psi_3^*(t),\psi_4^*(t)) = \min_{\Phi} J(\psi_1(t),\psi_2(t),\psi_3(t),\psi_4(t)) \quad (19)$$

where $\Phi = \psi_i(t), i = 1,2,3,4$ are lebesque measurable functions with $\psi_i(t) \in [0,1] : 0 \leq t \leq t_f$ Thus, Φ exists and it is bounded, closed and convex since the state and control variables are non-negative.

Thus, the Hamiltonian function is formulated by introducing the adjoint variables $\lambda_i(t), i = (S(t), V(t), E(t), A(t), I(t), Q(t), R(t), B_c(t))$ corresponding to the model's state variables. The Pontryagin minimum principle is then applied to derive the optimality system.

Theorem 5. *For the optimal control problem given by eqs. (17) and (18) with the initial conditions at $t = 0$, there exists $(\psi_1^*(t),\psi_2^*(t),\psi_3^*(t),\psi_4^*(t)) \in \mathbf{U}$ such that*

$$J(\psi_1^*(t),\psi_2^*(t),\psi_3^*(t),\psi_4^*(t)) = \min_{\Theta} J(\psi_1(t),\psi_2(t),\psi_3(t),\psi_4(t)),$$

where $\Theta = \psi_1(t),\psi_2(t),\psi_3(t),\psi_4(t) \in \mathbf{U}$.

Proof. In order to prove the results in Theorem 5, we adopt results in [54–56]. Thus, the following properties will be established

i The control set is convex and closed.

ii Non-negative solutions of the system (18) exists and it is bounded.

iii Since $\mathbf{U}$ contains all its limit points, the control set $\mathbf{U}$ is closed. Hence, given $\lambda \in [0,1]$ and any two arbitrary points $x, y \in \mathbf{U}$, where $\mathbf{x} = (\mathbf{x_1},\mathbf{x_2},\mathbf{x_3},\mathbf{x_4})$ and $\mathbf{y} = (\mathbf{y_1},\mathbf{y_2},\mathbf{y_3},\mathbf{y_4})$, then $\lambda\mathbf{x_i} + (1-\lambda)\mathbf{y_i} \in \mathbf{U}$ for $i = 1,2,3,4$ satisfying the convexity property of the control set.

iv Given the initial conditions $\mathbf{N}(0) \geq 0$, for $\mathbf{N}(t) = (S(t), V(t), E(t), A(t), I(t), Q(t), R(t), B_c(t)) \in R^8_+$, there exists a non-negative bounded optimal control problem and controls that are lebesgue measurable. It is noted that the OCP given by system (18) can be written as:

$$\frac{d\mathbf{Y}}{dt} = \mathbf{D}(\psi)\mathbf{Y} + \mathbf{G}(\psi,\mathbf{Y}) \quad (20)$$

where

$$\mathbf{Y}(t) = (S(t), V(t), E(t), A(t), I(t), Q(t), R(t), B_c(t))^T,$$

$$\mathbf{D}(\psi) = \begin{pmatrix} J_1 & 0 & 0 & 0 & 0 & 0 & \omega & 0 \\ 0 & \mathbf{d_1} & 0 & 0 & 0 & 0 & 0 & 0 \\ 0 & 0 & J_4 & 0 & 0 & 0 & 0 & 0 \\ 0 & 0 & \tau\sigma_1 & -\mathbf{d_1} & 0 & 0 & 0 & 0 \\ 0 & 0 & J_8 & \psi_3\sigma_2 & -\mathbf{d_2} & 0 & 0 & 0 \\ 0 & 0 & 0 & 0 & \eta & -\mathbf{d_3} & 0 & 0 \\ 0 & 0 & 0 & \gamma_1 & \gamma_2 & \gamma_3 & J_{11} & 0 \\ 0 & 0 & 0 & \bar{\psi}_4\rho_1 & \bar{\psi}_4\rho_2 & \bar{\psi}_4\rho_3 & 0 & -\mu_c \end{pmatrix},$$

$$\mathbf{G}(\psi, \mathbf{Y}) = \begin{pmatrix} \alpha_h - (1-\psi_1)\,\mathbf{d_5} \\ -\psi_2\mathbf{d_5} \\ (1-\psi_1)\,\mathbf{d_5} + \psi_2\,(1-\epsilon)\left(\frac{\beta_h(\pi A+i)}{N} + \frac{\beta B_c}{C+B_c}\right) \\ 0 \\ 0 \\ 0 \\ 0 \\ \alpha\left(1-\frac{B_c}{C}\right)B_c \end{pmatrix},$$

$$\mathbf{d_1} = \nu - \mu,$$

$$\mathbf{d_2} = \psi_3\sigma_2 + \gamma_1 + \mu,$$

$$\mathbf{d_3} = \eta + \gamma_2 + \delta + \mu,$$

$$\mathbf{d_4} = \gamma_3 + \delta + \mu,$$

$$\mathbf{d_5} = \frac{\beta_h\,(\pi A + I)}{N} + \frac{\beta B_c}{C + B_c}.$$

Equation (20) is a non-linear coupled system with bounded coefficients. Let

$$\mathbf{H}(\mathbf{Y}) = \mathbf{D}\mathbf{Y} + \mathbf{G}(\psi, \mathbf{Y}) \tag{21}$$

Hence, it can be seen from the first equation of eq. (18) that

$$\begin{aligned} \mathbf{G}(\psi, \mathbf{Y_1}) - \mathbf{G}(\psi, \mathbf{Y_2}) = &\Big\{ -(1-\psi_1(t))\frac{S_1(t)}{N_1(t)}\big(\beta_h(\pi A_1(t) \\ &+ I_1(t))\big)\Big\} - \Big\{ -\big(\beta_h(\pi A_2(t) \\ &+ I_2(t))\big)(1-\psi_1(t))\frac{S_2(t)}{N_2(t)}\Big\}, \\ |\mathbf{G}(\psi, \mathbf{Y_1}) - \mathbf{G}(\psi, \mathbf{Y_2})| \le &\Big| -(1-\psi_1(t))\frac{S_1(t)}{N_1(t)}\big((\beta_h(\pi A_1(t) \\ &+ I_1(t))) - (\beta_h(\pi A_2(t) + I_2(t)))\big)\Big|, \\ |\mathbf{G}(\psi, \mathbf{Y_1}) - \mathbf{G}(\psi, \mathbf{Y_2})| \le &\Big|(1-\psi_1(t))\frac{S_1(t)}{N_1(t)}\Big|\big(|\beta_h|\,|\pi|\,|A_1(t) \\ &- A_2(t)| + |\beta_h|\,|I_1(t) - I_2(t)|\big), \end{aligned}$$

and

$$\begin{aligned} \mathbf{D}Y_1 - \mathbf{D}Y_2 = &\{-(\nu+\mu)S_1 + \omega R_1\} - \{-(\nu+\mu)S_2 \\ &+ \omega R_2\}, \\ |\mathbf{D}Y_1 - \mathbf{D}Y_2| \le &\,|\nu+\mu|\,|S_1 - S_2| + |\omega|\,|R_1 - R_2|. \end{aligned}$$

Similarly, eq. (21) becomes

$$\begin{aligned} |\mathbf{H}(\mathbf{Y_1}) - \mathbf{H}(\mathbf{Y_1})| \le &\,|\nu+\mu|\,|S_1 - S_2| + |\omega|\,|R_1 - R_2|, \\ |\mathbf{G}(\psi, \mathbf{Y_1}) - \mathbf{G}(\psi, \mathbf{Y_2})| \le &\Big|(1-\psi_1(t))\frac{S_1(t)}{N_1(t)}\Big|\big(|\beta_h|\,|\pi|\,|A_1(t) \\ &- A_2(t)| + |\beta_h|\,|I_1(t) - I_2(t)|\big). \end{aligned}$$

□

The following optimality system is derived by adopting the approach in [14, 44, 45, 52, 57–59]:

Theorem 6. *Given the optimal control $\psi_1^*(t)$, $\psi_2^*(t)$, $\psi_3^*(t)$, $\psi_4^*(t)$ and solutions of the state variables $S^*(t)$, $V^*(t)$, $E^*(t)$, $A^*(t)$, $I^*(t)$, $Q^*(t)$, $R^*(t)$, $B_c^*(t)$, then there exists adjoint variables λ_i for*

$$i = (S(t), V(t), E(t), A(t), I(t), Q(t), R(t), B_c(t)),$$

that minimizes $J(\psi_1^*(t), \psi_2^*(t), \psi_3^*(t), \psi_4^*(t))$ over Φ satisfying:

$$\begin{aligned} \dot{\lambda_S} = &\,\lambda_S(\mu+\nu) - (\lambda_S - \lambda_E)\Bigg(\frac{\beta_h(I+\pi A)}{N} - \lambda_V\nu - (\psi_1 \\ &- 1)\left(\frac{\beta B_c}{B_c + C}\right) + \frac{\beta_h(I+\pi A)(\psi_1 - 1)S}{N^2}\Bigg) - (\lambda_E \\ &- \lambda_V)\left(\frac{\beta_h\psi_2(I+\pi A)(\varepsilon-1)V}{N^2}\right), \\ \dot{\lambda_V} = &\,\lambda_V\mu - (\lambda_V - \lambda_E)\Bigg(-\frac{\beta_h\psi_2(I+\pi A)(\varepsilon-1)V}{N^2} \\ &+ \psi_2\left(\frac{\beta B_c}{B_c + C} + \frac{\beta_h(I+\pi A)}{N}\right)(\varepsilon - 1)\Bigg) - (\lambda_E \\ &- \lambda_S)\left(\frac{\beta_h(I+\pi A)(\psi_1-1)S}{N^2}\right), \\ \dot{\lambda_E} = &\,(\lambda_E + \lambda_S)\left(\frac{\beta_h(I+\pi A)(\psi_1-1)S}{N^2}\right) - \lambda_A\sigma_1\tau - (\lambda_E \\ &- \lambda_V)\left(\frac{\beta_h\psi_2(I+\pi A)(\varepsilon-1)V}{N^2}\right) + \lambda_I\sigma_1(\tau-1), \\ \dot{\lambda_A} = &\,\lambda_A(\gamma_1 + \mu + \psi_3\sigma_2) - \lambda_R\gamma_1 - \kappa_1 - \lambda_{B_c}\psi_4\rho_1 - \lambda_I\psi_3\sigma_2 \\ &+ (\lambda_E - \lambda_S)\left((\psi_1 - 1)\left(\frac{\pi\beta_h}{N} - \frac{\beta_h(I+\pi A)}{N^2}\right)S\right) \\ &+ (\lambda_E - \lambda_V)\left(\psi_2(\varepsilon-1)\left(\frac{\pi\beta_h}{N} - \frac{\beta_h(I+\pi A)}{N^2}\right)V\right), \\ \dot{\lambda_I} = &\,\lambda_I(\delta + \eta + \gamma_2 + \mu) - \kappa_2 - \lambda_Q\eta - \lambda_R\gamma_2 - \lambda_{B_c}\psi_4\rho_2 \\ &+ (\lambda_E - \lambda_S)\left((\psi_1 - 1)\left(\frac{\pi\beta_h}{N} - \frac{\beta_h(I+\pi A)}{N^2}\right)\right)S \\ &+ (\lambda_E - \lambda_V)\left(\psi_2(\varepsilon-1)\left(\frac{\pi\beta_h}{N} - \frac{\beta_h(I+\pi A)}{N^2}\right)V\right), \\ \dot{\lambda_Q} = &\,-(\lambda_E - \lambda_S)\left(\left(\frac{\beta_h(I+\pi A)(\psi_1-1)}{N^2}\right)S - \lambda_R\gamma_3\right. \\ &\left.+ \left(\frac{\beta_h\psi_2(I+\pi A)(\varepsilon-1)}{N^2}\right)V\right)\lambda_Q(\delta + \gamma_3 + \mu) - \kappa_3, \\ \dot{\lambda_R} = &\,\lambda_R(\mu+\omega) - (\lambda_E - \lambda_S)\left(\frac{\beta_h(I+\pi A)(\psi_1-1)}{N^2}\right)S \\ &- (\lambda_E - \lambda_V)\left(\frac{\beta_h\psi_2(I+\pi A)(\varepsilon-1)}{N^2}\right)V - \lambda_S\omega, \\ \dot{\lambda_{B_c}} = &\,-\kappa_4 - (\lambda_E - \lambda_S)(\psi_1 - 1)\left(\frac{\beta B_c}{(B_c+C)^2} - \frac{\beta}{(B_c+C)}\right) \end{aligned} \tag{22}$$

$$+\frac{\beta_h(I+\pi A)}{N^2}\Big)S+\lambda_{B_c}\left(\mu_c+\alpha\left(\frac{B_c}{C}-1\right)+\frac{\alpha B_c}{C}\right)$$
$$-(\lambda_E-\lambda_V)\psi_2(\varepsilon-1)\left(\frac{\beta B_c}{(B_c+C)^2}-\frac{\beta}{(B_c+C)}\right.$$
$$\left.+\frac{\beta_h(I+\pi A)}{N^2}\right)V,$$

with the control variables $\psi_1^*(t),\psi_2^*(t),\psi_3^*(t),\psi_4^*(t)$ *and the transversality conditions*

$$\lambda_i(t_f)=0,\ i=(S(t),V(t),E(t),A(t),I(t),Q(t),R(t),B_c(t)). \tag{23}$$

The characterization of the control variables is presented by the following optimality conditions:

$$\psi_1^*(t)=\min\left\{1,\max\left\{0,\left(\frac{(\lambda_E-\lambda_S)}{\omega_1}\right)\mathbf{d_5}S\right\},1\right\}$$
$$\psi_2^*(t)=\min\left\{1,\max\left\{0,\frac{(\lambda_E-\lambda_V)(\varepsilon-1)}{\omega_2}\mathbf{d_5}V\right\},1\right\}$$
$$\psi_3^*(t)=\min\left\{1,\max\left\{0,\frac{(\lambda_A-\lambda_I)\sigma_2 A}{\omega_3}\right\},1\right\}$$
$$\psi_4^*(t)=\min\left\{1,\max\left\{0,\frac{\lambda_{B_c}(\rho_1A+\rho_2I+\rho_3Q)}{\omega_4}\right\},1\right\}$$

Proof. Given the Hamiltonian function, **H**, defined explicitly as

$$\mathbf{H}=\kappa_1A(t)+\kappa_2I(t)+\kappa_3Q(t)+\kappa_4B_c(t))+\frac{1}{2}\omega_1\psi_1^2(t)+\frac{1}{2}\omega_2\psi_2^2(t)$$
$$+\frac{1}{2}\omega_3\psi_3^2(t)+\frac{1}{2}\omega_4\psi_4^2(t)+\lambda_S\Big(\alpha_h+\omega R(t)-\nu S(t)-(1$$
$$-\psi_1(t))\left(\frac{\beta_h(\pi A(t)+I(t))}{N(t)}+\frac{\beta B_c(t)}{C+B_c(t)}\right)S(t)-\mu S(t)\Big)$$
$$+\lambda_V\Big(-\psi_2(t)(1-\varepsilon)\left(\frac{\beta_h(\pi A(t)+I(t))}{N(t)}+\frac{\beta B_c(t)}{C+B_c(t)}\right)V(t)$$
$$-\mu V(t)+\nu S(t)\Big)+\lambda_E\Big((1-\psi_1(t))\Big(\frac{\beta_h(\pi A(t)+I(t))}{N(t)}$$
$$+\frac{\beta B_c(t)}{C+B_c(t)}\Big)S(t)+\psi_2(t)(1-\varepsilon)\Big(\frac{\beta_h(\pi A(t)+I(t))}{N(t)}$$
$$+\frac{\beta B_c(t)}{C+B_c(t)}\Big)V(t)-\sigma_1E(t)-\mu E(t)\Big)+\lambda_A\big(\tau(t)\sigma_1E(t)$$
$$-\psi_3(t)\sigma_2A(t)-\gamma_1A(t)-\mu A(t)\big)+\lambda_I\big((1-\tau)\sigma_1E(t)-\eta I(t)$$
$$+\psi_3(t)\sigma_2A(t)-\gamma_2I(t)-\delta I(t)-\mu I(t)\big)+\lambda_Q\big(\eta I(t)-\gamma_3Q(t)$$
$$-\delta Q(t)-\mu Q(t)\big)+\lambda_R\big(\gamma_1A(t)+\gamma_2I(t)+\gamma_3Q(t)-\omega R(t)$$
$$-\mu R(t)\big)+\lambda_{B_c}\Big(\alpha\Big(1-\frac{B_c(t)}{C}\Big)B_c(t)+\psi_4(t)(\rho_1A(t)+\rho_2I(t)$$
$$+\rho_3Q(t))-\mu_cB_c(t)\Big),$$

the adjoint system is obtained by taking the partial derivatives of the Hamiltonian function, **H**, with respect to each state variable of the model:

$$\dot{\lambda_S}=-\frac{\partial\mathbf{H}}{\partial S(t)},\quad \lambda_S(f_f)=0,$$
$$\dot{\lambda_V}=-\frac{\partial\mathbf{H}}{\partial V(t)},\quad \lambda_V(f_f)=0,$$
$$\dot{\lambda_E}=-\frac{\partial\mathbf{H}}{\partial E(t)},\quad \lambda_E(f_f)=0,$$
$$\dot{\lambda_A}=-\frac{\partial\mathbf{H}}{\partial A(t)},\quad \lambda_A(f_f)=0,$$
$$\dot{\lambda_I}=-\frac{\partial\mathbf{H}}{\partial I(t)},\quad \lambda_I(f_f)=0,$$
$$\dot{\lambda_Q}=-\frac{\partial\mathbf{H}}{\partial Q(t)},\quad \lambda_Q(f_f)=0,$$
$$\dot{\lambda_R}=\frac{\partial\mathbf{H}}{\partial R(t)},\quad \lambda_R(f_f)=0,$$
$$\dot{\lambda_{B_c}}=\frac{\partial\mathbf{H}}{\partial B_c(t)},\quad \lambda_{B_c}(f_f)=0,$$

□

From the optimality conditions, if (x,ψ) is the optimal solution of the given optimal control problem, then $\frac{\partial\mathbf{H}}{\partial\psi_1}=\frac{\partial\mathbf{H}}{\partial\psi_2}=\frac{\partial\mathbf{H}}{\partial\psi_3}=\frac{\partial\mathbf{H}}{\partial\psi_4}=0$ at $\psi_i=\psi_i^*$

$$\frac{\partial\mathbf{H}}{\partial\psi_1}=\omega_1\psi_1+(\lambda_S-\lambda_E)\mathbf{d_5}S,$$
$$\frac{\partial\mathbf{H}}{\partial\psi_2}=\omega_2\psi_2+(\lambda_V-\lambda_E)(\varepsilon-1)\mathbf{d_5}V,$$
$$\frac{\partial\mathbf{H}}{\partial\psi_3}=\omega_3\psi_3-(\lambda_A-\lambda_I)\sigma_2A,$$
$$\frac{\partial\mathbf{H}}{\partial\psi_4}=\omega_4\psi_4+\lambda_{B_c}(\rho_1A+\rho_2I+\rho_3Q).$$

Hence, the optimal control functions are given as

$$\psi_1^*=\frac{(\lambda_E-\lambda_S)}{\omega_1}\mathbf{d_5}S,$$
$$\psi_2^*=\frac{(\lambda_E-\lambda_V)(\varepsilon-1)}{\omega_2}\mathbf{d_5}V,$$
$$\psi_3^*=\frac{(\lambda_A-\lambda_I)\sigma_2A}{\omega_3} \tag{24}$$
$$\psi_4^*=\frac{\lambda_{B_c}(\rho_1A+\rho_2I+\rho_3Q)}{\omega_4}.$$

By the definition of standard control and using the bounds on ψ_i^*, we obtain

$$\psi_i^*=\begin{cases}0,\ \text{if}\ \vartheta_i^*\le 0,\\ \vartheta_i^*,\ \text{if}\ 0<\vartheta_i^*<1,\\ 1,\ \text{if}\ \vartheta_i^*\ge 0.\end{cases}$$

where $i=1,2,3,4$ and

$$\vartheta_1=\frac{(\lambda_E-\lambda_S)}{\omega_1}\mathbf{d_5}S.$$

Hence, the control for the personal protection, ψ_1, can be written in compact form as

$$\psi_1^*(t)=\min\left\{1,\max\left\{0,\vartheta_1\right\}\right\}.$$

Similarly,

$$\vartheta_2=\frac{(\lambda_E-\lambda_V)(\varepsilon-1)}{\omega_2}\mathbf{d_5}V.$$

Thus, the control for booster vaccine administration, ψ_2, can be

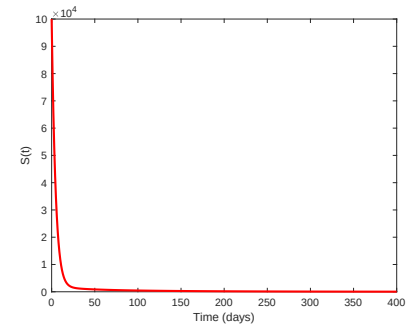

(a) Susceptible Humans

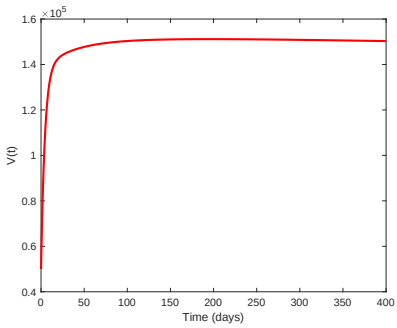

(b) Vaccinated Humans

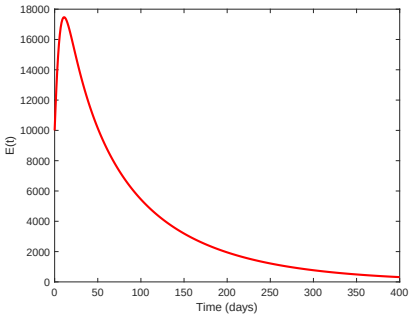

(c) Exposed Humans

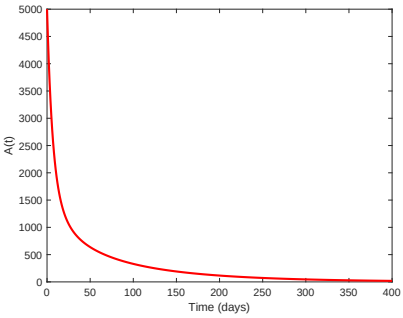

(d) Asymptomatic Infected Humans

Figure 2. Evolution of $S(t)$, $V(t)$, $E(t)$ and $A(t)$ Subpopulations

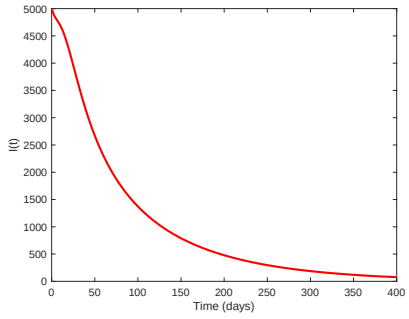

(a) Infected Humans

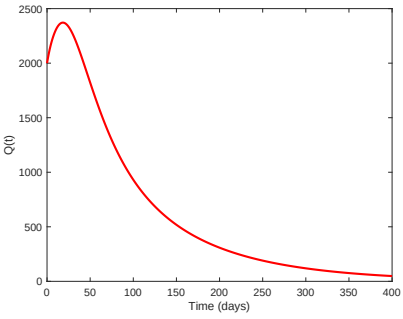

(b) Quarantined Humans

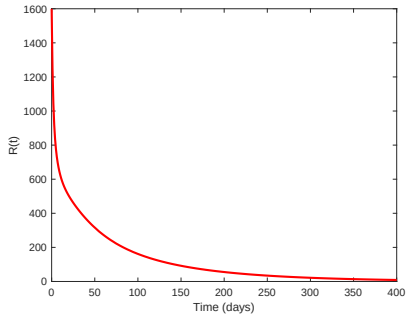

(c) Recovered Humans

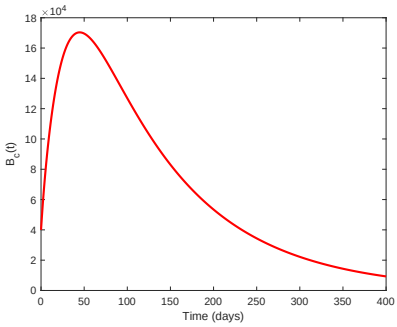

(d) Bacteria concentration in the environment

Figure 3. Evolution of $I(t)$, $Q(t)$, $R(t)$ and $B_c(t)$ Subpopulations

written in compact form as

$$\psi_2^*(t) = \min\{1, \max\{0, \vartheta_1\}\}.$$

In addition,

$$\vartheta_3 = \frac{(\lambda_A - \lambda_I)\sigma_2 A}{\omega_3}.$$

Therefore, the control for the preventive strategies employed to detect and treat asymptomatic infected humans, ψ_3, can be written in compact form as

$$\psi_3^*(t) = \min\{1, \max\{0, \vartheta_3\}\}.$$

Lastly,

$$\vartheta_4 = \frac{\lambda_{B_c}(\rho_1 A + \rho_2 I + \rho_3 Q)}{\omega_4}.$$

The compact form of the control that represents all efforts by medical personnel and health authorities to reduce diphtheria bacteria concentration, ψ_4, can be written as

$$\psi_4^*(t) = \min\{1, \max\{0, \vartheta_4\}\}.$$

4. Results and Discussion

This section examines the dynamic behaviour of the diphtheria system (2). Numerical simulations are used to solve the resulting two-point boundary value problem for a sixteen-dimensional optimality system. These simulations are conducted using MATLAB with the ode45 solver. The initial conditions for the model are as follows

$$(S_0, V_0, E_0, A_0, I_0, Q_0, \mathbb{R}_0, B_{c0}) = (100000, 50000, 10000, 5000, 5000, 2000, 1600, 40000).$$

4.1. Autonomous System

The values of the parameters for the simulation of the proposed diphtheria model are given in subsection 2.4 and the calculated $\mathbb{R}_0$ of the system (2) is approximately $\mathbb{R}_0 = 1.5103$.

Figures 2 and 3 present the results of the numerical simulation of each model compartment of system (2) over a period of 400 days. Figure 2a shows that the interactions between susceptible and infected individuals together with the introduction of vaccination lead to a rapid decrease in the susceptible class. However, a stationary point is attained after about 50 days. This is largely due to the progression of susceptible individuals to vaccinated and exposed classes. Conversely, the initial days see a rapid increase in the vaccinated population, driven by heightened awareness and the urgent need to get people vaccinated. Thereafter, the vaccinated class attains near a steady state after about 90 days (see Figure 2b). Figure 2c indicates that the exposed population increases sharply at the initial stage as a result of interactions between susceptible and infected individuals. Then, this class begins to decrease drastically as a result of progression of individuals to the asymptomatic infected class. The asymptomatic infected group declines rapidly due to individuals progressing to the symptomatic stage, as well as the natural recovery of many within this group as indicated in Figure 2d. Figure 3a reveals a continuous decline in the number of individuals infected with diphtheria due to the efficacy of the vaccines and natural recovery of the asymptomatic individuals. Figure 3b reveals a slight increase in the number individuals that are placed in a quarantine. This population begins to reduce as a result of the decline in the number of infected individuals. In view of Figures 3a and 3b, there is a sharp reduction in the number of people that recover from diphtheria as shown in Figure 3c. Figure 3d indicates a sharp increase in the bacteria concentration in the environment for the first 60 days. Thereafter, this population begins to decline as a results of the reduction in the number of individuals in the $A(t)$, $I(t)$ and $Q(t)$ classes.

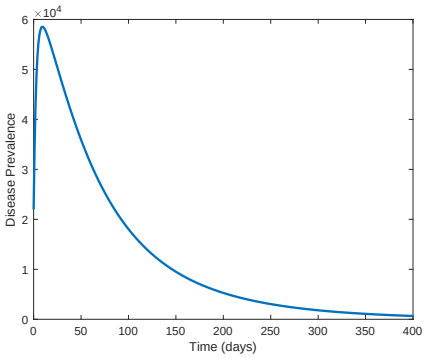

Figure 4. Disease Prevalence

Figure 4 shows a rapid increase in diphtheria prevalence in the first 10 days of the introduction of the control strategy. Thereafter, the disease prevalence begins to decline as a results of the efficacy of the vaccine and the reduction in the asymptomatic, infected and quarantined subpopulations.

Figure 5a shows that an increase in the vaccination rate (ν) of individuals in the susceptible class leads to an increase in the number of people that are vaccinated against diphtheria. On the other hand, Figures 5b and 5f reveal that an increase in the vaccination rate results in a decrease in the number of individuals in the $E(t)$, $A(t)$, $I(t)$, $Q(t)$ and $R(t)$ subpopulations. This reveals the effectiveness of vaccines in curtailing the spread of diphtheria infection.

4.2. Non-autonomous System

The sixteen-dimensional optimality system is solved through an iterative forward-backward sweep method (FBSM), coupled with the fourth-order Runge-Kutta algorithm and implemented in MATLAB. This system represents a two-point boundary value problem, which consists of the state system (2), the adjoint system (22), and the control eq. (24) defined over the time interval $[0, 400]$ days. Our goal is to determine the optimal control strategies needed to mitigate the spread of diphtheria epidemic within the population.

Due to the differing time orientations of the optimality system given by the equations of the non-autonomous system (18) are solved forward in time, starting with initial conditions and an initial guess for the control. In contrast, the equations of the adjoint system (22), with terminal conditions (23), are solved backward in time, using the current iteration solution from the state system [52].

The weight constants κ_i and ψ_i where $i = 1, 2, 3$ and 4 associated with the objective functional (17), along with the parameter values in subsection 2.4, are taken as follows: $\kappa_1 = 0.025, \kappa_2 = 0.020, \kappa_3 = 0.005, \kappa_4 = 0.001, \psi_1 = 250, \psi_2 =$

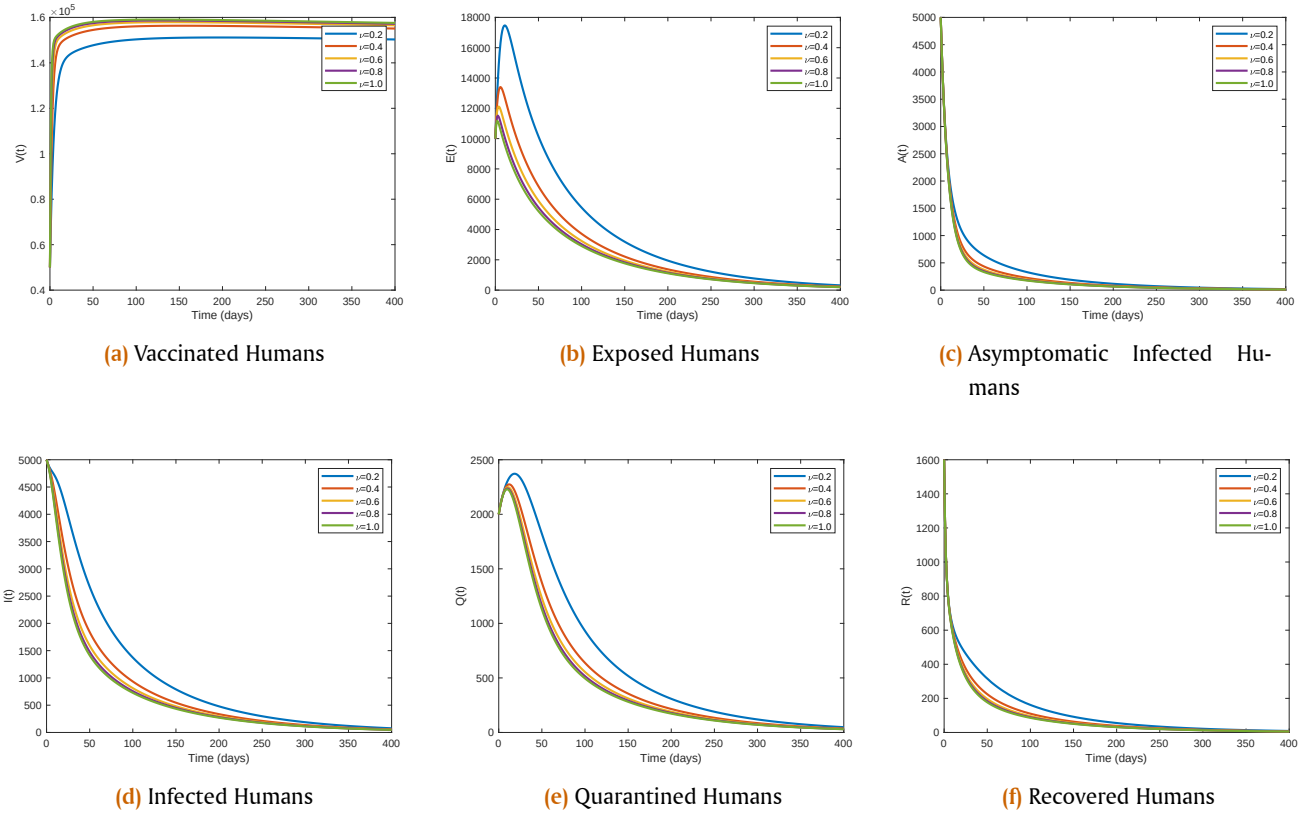

(a) Vaccinated Humans **(b)** Exposed Humans **(c)** Asymptomatic Infected Humans

(d) Infected Humans **(e)** Quarantined Humans **(f)** Recovered Humans

Figure 5. Simulation showing the effects of vaccination rate (ν) on $V(t)$, $E(t)$, $A(t)$, $I(t)$, $Q(t)$ and $R_h(t)$ Compartments

$150, \psi_3 = 100$ and $\psi_4 = 200$. These weights are taken theoretically mainly for the the numerical simulations of the proposed optimal control problem.

In order to optimize the objective functional (17), different combinations of the optimal control strategies are examined. The combinations of four different control strategies are examined. We note that each of these strategies involves at least three optimal controls. The strategies are:

- Strategy A: A combination of optimal personal protection, detection/treatment of the asymptomatic infected humans and reduction of bacteria concentration (i.e. $\psi_1(t), \psi_3(t)$ and $\psi_4(t)$ with $\psi_2(t) = 0$),
- Strategy B: A combination of optimal personal protection, booster vaccine administration and reduction of bacteria concentration (i.e. $\psi_1(t), \psi_2(t)$ and $\psi_4(t)$ with , $\psi_3(t) = 0$),
- Strategy C: A combination of optimal personal protection, booster vaccine administration and detection/treatment of the asymptomatic infected humans (i.e. $\psi_1(t), \psi_2(t)$ and $\psi_3(t)$ with $\psi_4(t) = 0$) and
- Strategy D: A combination of optimal personal protection, booster vaccine administration, detection/treatment of the asymptomatic infected humans and reduction of bacteria concentration (i.e. $\psi_1(t), \psi_2(t), \psi_3(t)$ and $\psi_4(t)$)

According to World Health Organization release [1], personal protection, $\psi_1(t)$, such as avoiding contact with individuals that have symptoms of diphtheria, frequent hand washing with soap and water, the use of nose masks or covering one's mouth and nose with tissue especially when coughing is a major means of preventing the disease. Hence, this preventive measure is included in each of the four control strategies considered in this research.

1. strategy A: a combination of optimal personal protection, detection/treatment of the asymptomatic infected humans and reduction of bacteria concentration (i.e. $\psi_1(t), \psi_3(t)$ and $\psi_4(t)$ with $\psi_2(t) = 0$).
   Figure 6 shows the effects of a combination of optimal personal protection, detection/treatment of the asymptomatic infected humans and reduction of bacteria concentration (i.e. $\psi_1(t), \psi_3(t)$ and $\psi_4(t)$ with $\psi_2(t) = 0$) on the optimal control problem. Figure 6a shows a reduction in the number of individuals infected with diphtheria when the three controls are implemented together than the scenario without control. For the quarantined subpopulation, the controlled system indicates that lesser number of people will need to be placed in a quarantine when compared with the uncontrolled system (see Figure 6b). In view of Figures 6a and 6b, Figure 6c reveals that there is a reduction in the magnitude of individuals that recover from the disease in the presence of the three controls measures relative to the case without control. Figure 6d shows a drastic decrease in the size of the people that have diphtheria infection for the situation where these control measures are applied to the system as against the instance without control. The control profile given in Figure 6e shows that the optimal controls ψ_2 and ψ_3 should be maintained at full coverage in the first 130 days before gradually declining to a minimal level towards the end of the control implementation period. On the other hand, optimal controls ψ_1 should be sustained for the initial 160 days from

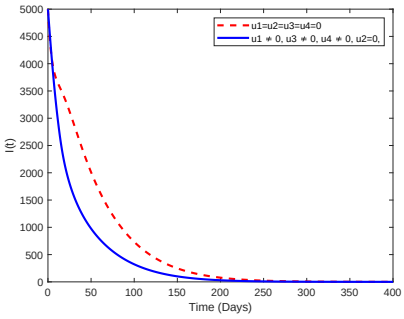

(a) Infected Humans

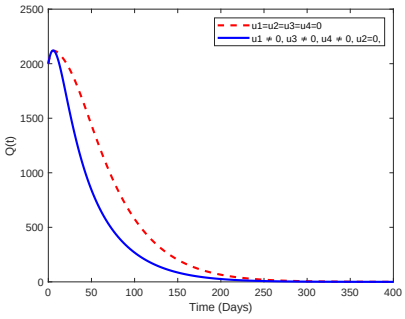

(b) Quarantined Humans

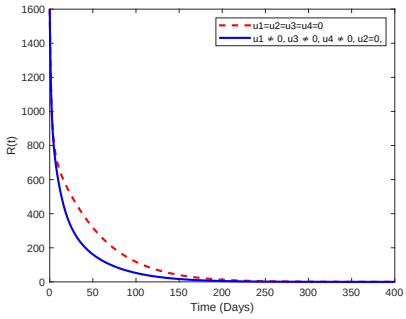

(c) Recovered Humans

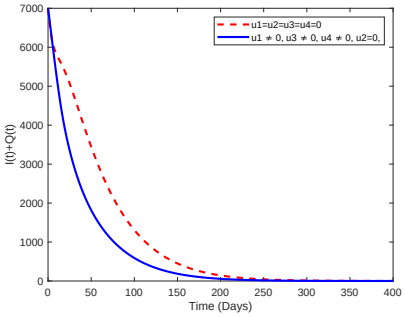

(d) Disease Prevalence

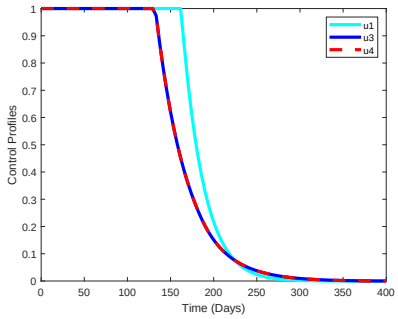

(e) Control Profiles

Figure 6. Effects of strategy A on Diphtheria Population Dynamics

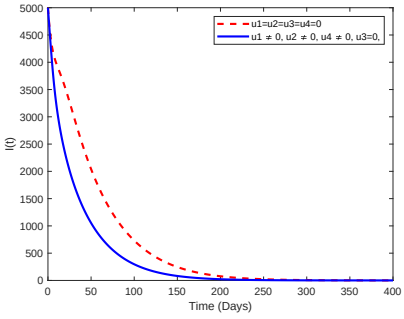

(a) Infected Humans

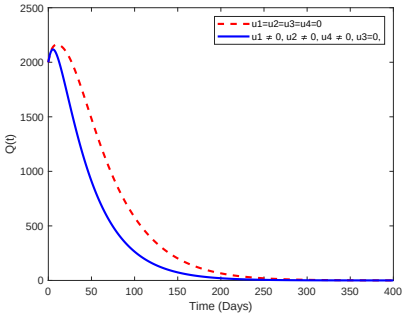

(b) Quarantined Humans

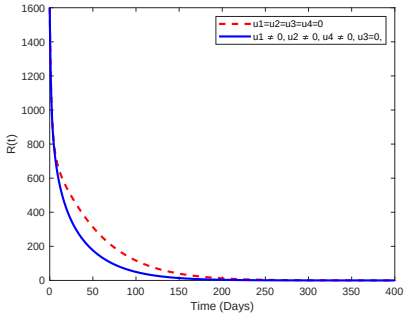

(c) Recovered Humans

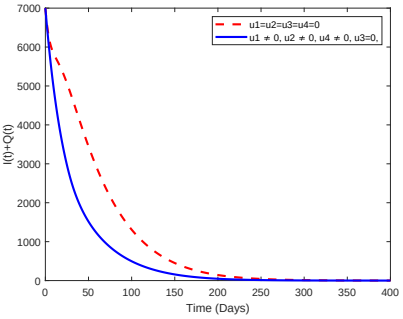

(d) Disease Prevalence

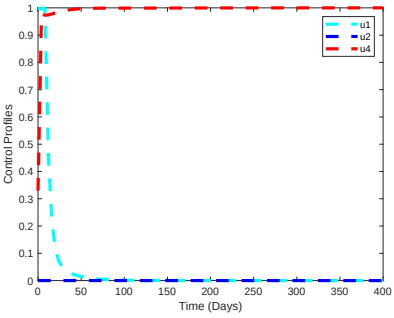

(e) Control Profiles

Figure 7. Effects of strategy B on Diphtheria Population Dynamics

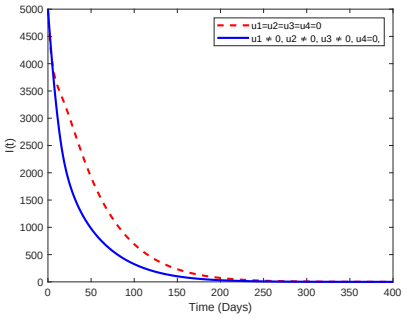

(a) Infected Humans

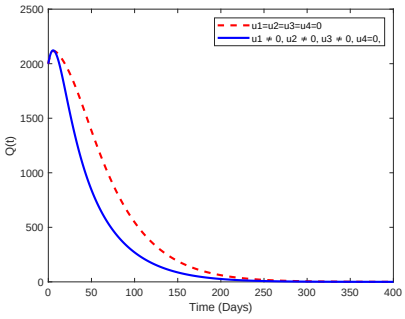

(b) Quarantined Humans

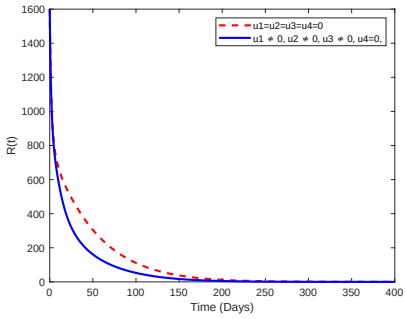

(c) Recovered Humans

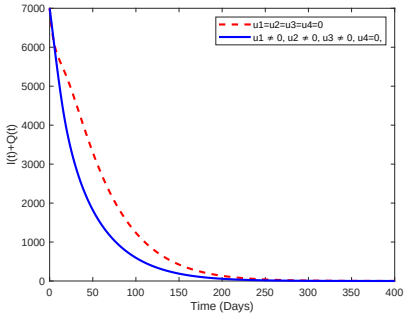

(d) Disease Prevalence

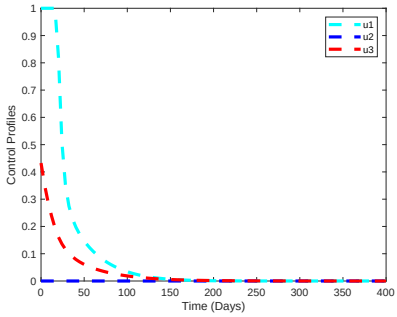

(e) Control Profiles

Figure 8. Effects of strategy C on Diphtheria Population Dynamics

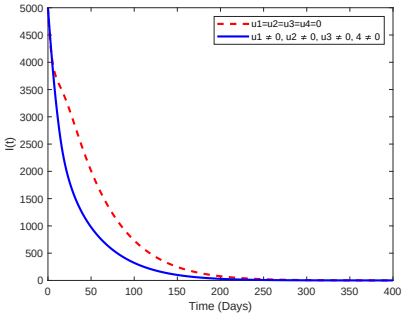

(a) Infected Humans

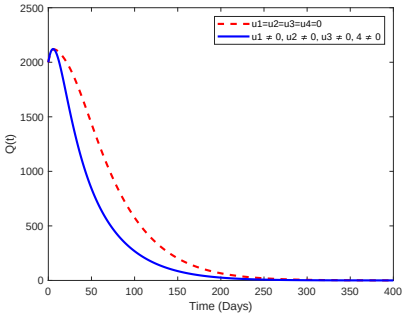

(b) Quarantined Humans

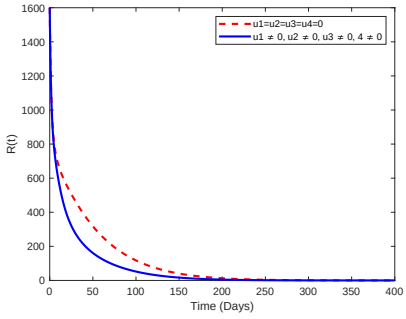

(c) Recovered Humans

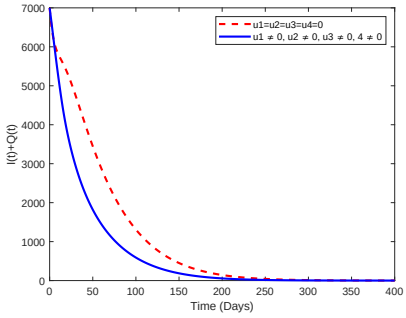

(d) Disease Prevalence

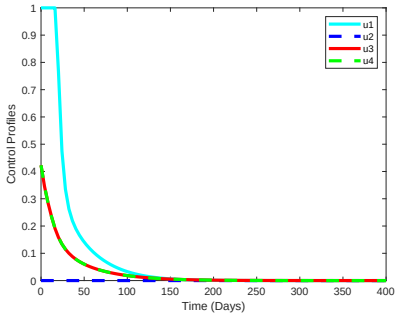

(e) Control Profiles

Figure 9. Effects of strategy D on Diphtheria Population Dynamics

Table 3. Strategy, Total Infections Averted, Total Cost, IAR and ACER

Strategy	Total Infection Averted	Total Cost ($)	IAR	ACER
$A : \psi_1(t), \psi_3(t), \psi_4(t)$	156107.04	3180.16	0.3698	0.0120
$B : \psi_1(t), \psi_2(t), \psi_4(t)$	161031.81	41091.04	0.3716	0.1509
$C : \psi_1(t), \psi_2(t), \psi_3(t)$	140758.52	3153.61	0.3455	0.0118
$D : \psi_1(t), \psi_2(t), \psi_3(t), \psi_4(t)$	199093.07	21791.89	0.4716	0.0977

Table 4. Strategy, Total Infections Averted, Total Cost, IAR and ICER

Strategy	Total Infection Averted	Total Cost ($)	ICER
$C : \psi_1(t), \psi_2(t), \psi_3(t)$	140758.52	3153.61	0.0224
$A : \psi_1(t), \psi_3(t), \psi_4(t)$	156107.04	3180.16	0.0017
$B : \psi_1(t), \psi_2(t), \psi_4(t)$	161031.81	41091.04	7.6981
$D : \psi_1(t), \psi_2(t), \psi_3(t), \psi_4(t)$	199093.07	21791.89	–0.5072

Table 5. Performance Comparison of Strategies C and D

Strategy	Total Infection Averted	Total Cost ($)	ICER
$C : \psi_1(t), \psi_2(t), \psi_3(t)$	140758.52	3153.61	0.0224
$A : \psi_1(t), \psi_3(t), \psi_4(t)$	156107.04	3180.16	0.00173
$D : \psi_1(t), \psi_2(t), \psi_3(t), \psi_4(t)$	199093.07	21791.89	0.4330

Table 6. Performance Comparison of Strategies C and A

Strategy	Total Infection Averted	Total Cost ($)	ICER
$C : \psi_1(t), \psi_2(t), \psi_3(t)$	140758.52	3153.61	0.0224
$A : \psi_1(t), \psi_3(t), \psi_4(t)$	156107.04	3180.16	0.00173

the date of the commencement of the introduction of the control strategy before observing a steady decline towards the lower bounds till the final time.

2. strategy B: a combination of optimal personal protection, booster vaccine administration and reduction of bacteria concentration (i.e. $\psi_1(t), \psi_2(t)$ and $\psi_4(t)$ with, $\psi_3(t) = 0$). Effects of the combination of optimal personal protection, booster vaccine administration and reduction of bacteria concentration (i.e. $\psi_1(t), \psi_2(t)$ and $\psi_4(t)$ with , $\psi_3(t) = 0$) are examined as shown in Figure 7. Figure 7a illustrates a reduction in the number of individuals infected with diphtheria when all the three control measures are implemented, compared to the scenario without any controls. For the quarantined subpopulation, the controlled system shows that fewer people will require quarantine, in contrast to the uncontrolled system (see Figure 7b). In light of Figures 7a and 7b, Figure 7c indicates a reduction in the number of individuals recovering from the disease when the three control measures are applied, compared to the case without controls. Figure 7d demonstrates a significant decrease in the prevalence of diphtheria when these control measures are enforced, as opposed to the scenario without any intervention. The control profile presented in Figure 7e suggests that $\psi_4(t)$ Should be maintained at full coverage level throughout the intervention period. The optimal control $\psi_1(t)$ should be maintained at the highest level for the first 10 days after the introduction of strategy B. Thereafter, the control measure can be relaxed gradually before falling to the lowest level after about 75 days while the control profile $\psi_2(t)$ could be left at the lowest level throughout the period of this intervention.
3. strategy C: a combination of optimal personal protection, booster vaccine administration and detection/treatment of the asymptomatic infected humans (i.e. $\psi_1(t), \psi_2(t)$ and $\psi_3(t)$ with $\psi_4(t) = 0$).
Figure 8 illustrates the effects of the combination of optimal personal protection, booster vaccine administration and detection/treatment of the asymptomatic infected humans (i.e. $\psi_1(t), \psi_2(t)$ and $\psi_3(t)$ with $\psi_4(t) = 0$). Figure 8a depicts a notable decline in the number of individuals infected with diphtheria under the implementation of all the three control strategies, compared to the baseline scenario without control measures. For the quarantined subpopulation, the controlled system indicates a lower proportion of individuals requiring quarantine, as opposed to the uncontrolled system (see Figure 8b). Figure 8c demonstrates a reduction in the number of recoveries when the control strategies are applied, relative to the no-control scenario. Figure 8d highlights a substantial decrease in the prevalence of diphtheria under the implementation of the control measures, compared to the uncontrolled case. The control profile depicted in Figure 8e suggests that $\psi_1(t)$ should be sustained at full coverage for the initial 15 days, while $\psi_3(t)$ should be applied at approximately 45% at the commencement of the intervention. On the other hand, the optimal control $\psi_2(t)$ could be sustained at its lowest level throughout the intervention period.
4. strategy D: a combination of optimal personal protection, booster vaccine administration, detection/treatment of the asymptomatic infected humans and reduction of bacteria concentration (i.e. $\psi_1(t), \psi_2(t), \psi_3(t)$ and $\psi_4(t)$).
Figure 9 demonstrates the dynamics of the system under the combined influence of optimal personal protection, booster vaccine administration, detection/treatment of the asymptomatic infected humans and reduction of bacteria concentration (i.e. $\psi_1(t), \psi_2(t), \psi_3(t)$ and $\psi_4(t)$). As depicted in

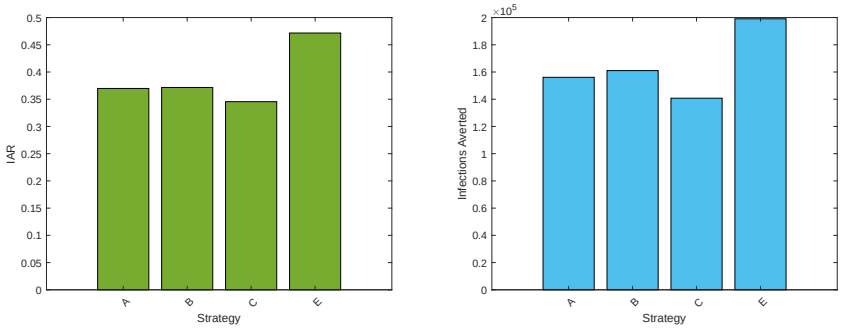

(a) Plots of Infection Averted Ratio for Strategies A, B, C and D

(b) Plots of Total Infection Averted for Strategies A, B, C and D

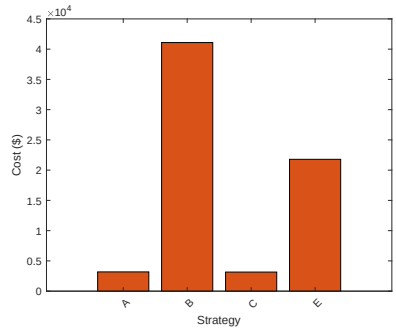

(c) Plots of Total Cost for Strategies A, B, C and D

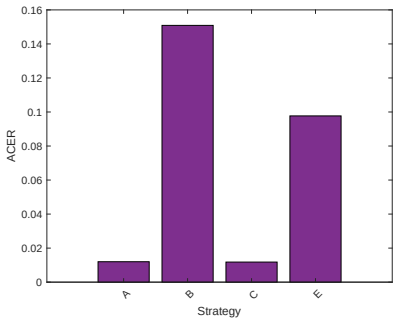

(d) Plots of ACER for Strategies A, B, C and D

Figure 10.

Figure 9a, there is a significant reduction in the infected population when all the four control strategies are simultaneously applied, in contrast to the uncontrolled baseline. The controlled model yields a lower proportion of individuals requiring quarantine relative to the uncontrolled model (see Figure 9b). Figure 9c illustrates a decline in the number of recoveries as a result of the applied control strategies, compared to the situation where no control is applied. Furthermore, Figure 9d reveals a marked reduction in the prevalence of diphtheria when the control interventions are implemented, compared to the scenario without interventions. The control profiles given in Figure 9e suggests that $\psi_1(t)$ should be maintained at maximum efficacy for the initial 15 days, while the optimal controls $\psi_2(t)$ and $\psi_3(t)$ should be applied at approximately 45% at the commencement of the implementation of the intervention strategy before gradually declining to the minimum level after about 130 days. The control variable $\psi_2(t)$ could remain at its minimal bound over the entire course of the intervention, ensuring minimal resource allocation towards this control variable.

4.3. Cost-Effectiveness Analysis

We proceeded with a cost-effectiveness analysis to assess the economic efficiency of various health interventions, such as personal protection, booster vaccine administration, detection/treatment of the asymptomatic infected humans and reduction of bacteria concentration. This type of analysis helps determine whether the health benefits gained justify the expenses involved. In this section, we evaluate three key metrics: the Infection Averted Ratio (IAR), the Average Cost-Effectiveness Ratio (ACER) and the Incremental Cost-Effectiveness Ratio (ICER) [60–68]

1. Infection Averted Ratio (IAR)
   The IAR is defined as:

$$\text{IAR} = \frac{\text{Total number of infection averted}}{\text{Total number of recovered}}.$$

   The number of infections prevented is calculated by subtracting the total number of infectious individuals under the control strategy from those in the absence of any control. The strategy that yields the highest reduction ratio is considered the most effective. This analytical method identifies the strategy with the highest IAR as offering the greatest cost-effectiveness [69–73]. The IAR for each strategy is computed using the parameter values in subsection 2.4. The results are shown in Table 3 and Figure 10a. Strategy D which involves a combination of optimal personal protection, booster vaccine administration, detection/treatment of the asymptomatic infected humans and reduction of bacteria concentration (i.e. $\psi_1(t), \psi_2(t), \psi_3(t)$ and $\psi_4(t)$) gives the highest IAR. Therefore, based on this cost analysis teechinique, strategy D is the most cost-effective. Strategy B considers a combination of optimal personal protection, booster vaccine administration and reduction of bacteria concentration (i.e. $\psi_1(t), \psi_2(t)$ and $\psi_4(t)$ with , $\psi_3(t) = 0$)

is the next cost effecitive. This is followed by Strategy A that combines optimal personal protection, detection/treatment of the asymptomatic infected humans and reduction of bacteria concentration (i.e. $\psi_1(t), \psi_3(t)$ and $\psi_4(t)$ with $\psi_2(t) = 0$). Strategy C gives the least cost-effective strategy and it involves optimal personal protection, booster vaccine administration and detection/treatment of the asymptomatic infected humans (i.e. $\psi_1(t), \psi_2(t)$ and $\psi_3(t)$ with $\psi_4(t) = 0$). Strategy C is the least cost-effective because it results in the smallest reduction in the number of infections within the population, as illustrated in Table 3 and Figure 10b.

2. Average Cost-Effectiveness Ratio
The Average Cost-Effectiveness Ratio (ACER) represents the cost required to prevent a single case of infection through a specific intervention. It is determined by dividing the overall cost of implementing the strategy by the total number of infections it successfully prevents.

$$\text{ACER} = \frac{\text{Total cost of implementing the strategy}}{\text{Total number of infections it successfully prevents}}. \tag{25}$$

The total cost produced by a strategy in view of the objective functional given in eq. (17) is expressed as

$$\text{TC} = \int_0^{t_f} (\kappa_1\psi_1 N + \kappa_2\psi_2 V + \kappa_3\psi_3 A + \kappa_4\psi_4 B_c + \omega_1\psi_1^2 + \omega_2\psi_2^2 + \omega_3\psi_3^2 + \omega_4\psi_4^2)dt. \tag{26}$$

A lower ACER value signifies a more efficient and economically favorable intervention [45, 60, 74–77]. Hence, eq. (25) is used to calculate the ACER for each of the four strategies. Table 4 and Figure 10d present the numerical results from the simulation.
Strategy C has the least ACER and based on this cost analysis technique, it is the most cost-effective method. It is followed by Strategy A and then Strategy D. Stragegy B has the highest ACER and hence, it is the least cost-effectiveness approach.
Further cost-effectiveness analysis are carried out in order to verify these results using the following approach.

3. Incremental Cost-Effectiveness Ratio
The Incremental Cost-Effectiveness Ratio (ICER) is used to measure how cost-effective a new health intervention is when compared to a baseline or standard approach. It is defined as

$$\begin{aligned} \text{ICER} &= \frac{e_1 - e_2}{e_3 - e_4}, \\ e_1 &= \text{Total cost with control}, \\ e_2 &= \text{Total cost without control}, \\ e_3 &= \text{Total number of infections without control}, \\ e_4 &= \text{Total number of infections with control}. \end{aligned} \tag{27}$$

Using the formula given by eq. (27) and the techniques in [64, 72, 78, 79], we compute the ICER for each of the strategies as follows:

$$\begin{aligned} \text{ICER(C)} &= \frac{3153.61}{140758.52} = 0.0224, \\ \text{ICER(A)} &= \frac{3180.16 - 3153.61}{156107.04 - 140758.52} = 0.0017, \\ \text{ICER(D)} &= \frac{21791.89 - 41091.04}{199093.07 - 161031.81} = -0.5072, \\ \text{ICER(B)} &= \frac{41091.04 - 3180.16}{161031.81 - 156107.04} = 7.6981. \end{aligned}$$

A comparison of Strategies C and B, in Table 4, shows that ICER(B) is greater than ICER(C). This reveals that Strategy B is dominated Strategy C. Hence, Strategy C has greater effectiveness at lower cost. Thus, Strategy B is excluded from subsequent analysis.
Furthermore, Startegy C is compared with Strategy D using eq. (27). The results of the analysis are presented in Table 5 and it shows that Strategy C has a lower ICER than Strategy D. This indicates that Strategy D is more expensive to implement and less cost-effective. Thus, Strategy D is removed from the set of interventions. Next, we are left with Startegy C and Strategy A. Again, using eq. (27), the summary of ICER for the two Strategies is give in Table 6. Table 6 reveals that Strategy A has a lower ICER than Strategy C. Thus, Strategy C is removeed from the list since Strategy A is more cost-effective than Strategy C. Therefore, Strategy A is the most cost-effective.
From the results of the cost-effectiveness analysis, Strategy A that combines optimal personal protection, detection/treatment of the asymptomatic infected humans and reduction of bacteria concentration (i.e. $\psi_1(t), \psi_3(t)$ and $\psi_4(t)$ with $\psi_2(t) = 0$) gives the smallest ICER and it is therefore the most cost-effective strategy. This agrees with the results in Figure 10c of the objective functional for each of the four strategies.

5. Conclusions

An autonomous system consisting of eight mutually exclusive classes - Susceptible, Vaccinated, Exposed, Asymptomatic, Symptomatic, Quarantined, Recovered and Bacteria concentration in the environment is formulated and analyzed. The fundamental properties of the model solutions are examined to establish its positivity and well-posedness. The disease-free equilibrium point of the model is proved to be LAS whenever $\mathbb{R}_0 < 1$ and unstable otherwise. Sensitivity analysis is performed in order to determine the relative importance of each of the model parameters influencing the transmission dynamics of diphtheria disease. For instance, the effects of vaccination rate, ν, on the transmission of the disease is examined. The results reveal that increasing the vaccination rate will drastically reduce the number of individuals that are asymptomatic, infected, quarantined and recover from the disease.

Based on the results of the sensitivity analysis, the model is extended into a non-autonomous system of sixteen ordinary differential equations. The proposed optimal control problem contains four time-varying controls: personal protection, booster vaccine administration, detection/treatment of the asymptomatic infected humans and reduction of bacteria concentration in the

environment. Pontryagin's maximum principle together with optimal control theory are used to analyze the optimal control problem. The impact of four distinct control strategies, each incorporating at least three of the control variables, is investigated to assess their influence on the transmission dynamics of the disease. The results reveal that each of the strategies A, B, C and D has the potential of drastically reducing the prevalence of diphtheria infection. In particular, by employing cost-effectiveness metrics-IAR, ACER and ICER, we identified Strategy A as the most economically efficient approach. This strategy, which integrates optimal personal protection, effective detection and treatment of asymptomatic individuals and reduction of environmental bacterial concentration offers the greatest potential for minimizing the disease burden at a sustainable cost. These findings provide valuable guidance for public health decision-makers aiming to implement impactful and cost-effective diphtheria control policies.

Author Contributions. **Afolabi, A. S.**: Conduct analysis and revise articles and perform numerical simulations. **Miswanto**: Responsible for revising and reviewing the analysis and overall structure of the article.

Acknowledgement.

1. The author would like to thank the Faculty of Science and Technology, Airlangga University for the facilities and academic support provided during the research.
2. The author would like to express his gratitude to the Airlangga Post Doctoral (APD) Fellowship, which has provided funding assistance for this research.
3. The authors sincerely thank the editors and reviewers for their valuable support and constructive feedback, which have greatly contributed to the improvement of this manuscript.

Funding. This research was funded by Airlangga Global Engagement (AGE) through the Airlangga Post-Doctoral Fellowship (APD) program.

Conflict of interest. The authors declare no conflict of interest.

Data availability. Not applicable.

References

[1] W. H. Organization, "Who african region health emergency situation report-multi-country outbreak of diphtheria, consolidated regional situation report number 006 – as of january 14, 2024," 2024, https://reliefweb.int/report/nigeria/who-african-region-health-emergency-situation-report-multi-country-outbreak-diphtheria-consolidated-regional-situation-report-006-january-14-2024, Accesed on 11 March 2025.

[2] L. Blumberg *et al.*, "The preventable tragedy of diphtheria in the 21st century," *International Journal of Infectious Diseases*, vol. 71, pp. 122–123, 2018.

[3] D. D. Gaiya *et al.*, "Diphtheria outbreak in nigeria: what we know now," *Infection Prevention in Practice*, vol. 6, no. 1, p. 100345, 2024. DOI:10.1016/j.infpip.2024.100345

[4] H. Husain, "An sir mathematical model for dipterid disease," in *Journal of Physics: Conference Series*, vol. 1280, no. 2, p. 022051, 2019. DOI:10.1088/1742-6596/1280/2/022051

[5] N. Kitamura, "Understanding factors contributing to outbreaks of diphtheria and implications for vaccination policy in vietnam [Dissertation]," London: London School of Hygiene & Tropical Medicine, 2023.

[6] D. Kolibo and S. Romaniuk, "Mathematical model of the infection process in diphtheria for determining the therapeutic dose of antitoxic anti-diphtheria serum," *Ukrains' kyi Biokhimichnyi Zhurnal*, vol. 73, no. 2, pp. 144–151, 2001.

[7] S. Latifah *et al.*, "Mathematical study for an infectious disease with awareness-based sis-m model," in *Journal of Physics: Conference Series*, vol. 1747, no. 1, p. 012017, 2021. DOI:10.1088/1742-6596/1747/1/012017

[8] M. Muscat *et al.*, "Diphtheria in the who european region, 2010 to 2019," *Eurosurveillance*, vol. 27, no. 8, p. 2100058, 2022. DOI:10.2807/1560-7917.ES.2022.27.8.2100058

[9] O. N. Olulaja *et al.*, "A looming epidemic: combating the recurrent outbreaks of diphtheria in nigeria," *The Pan African Medical Journal*, vol. 45, 2023. DOI:10.11604/pamj.2023.45.186.41328

[10] P. O. Omosigho *et al.*, "The re-emergence of diphtheria amidst multiple outbreaks in nigeria," *Infectious Disorders-Drug Targets*, vol. 24, no. 4, pp. 20–28, 2024. DOI:10.2174/0118715265251299231117045940

[11] S. Sharma and G. Samanta, "Stability analysis and optimal control of an epidemic model with vaccination," *International Journal of Biomathematics*, vol. 8, no. 3, p. 1550030, 2015. DOI:10.1142/S1793524515500308

[12] S. A. Truelove *et al.*, "Clinical and epidemiological aspects of diphtheria: a systematic review and pooled analysis," *Clinical Infectious Diseases*, vol. 71, no. 1, pp. 89–97, 2020. DOI:10.1093/cid/ciz808

[13] S. S. Voss *et al.*, "Underreporting of the 5-year tetanus, diphtheria, pertussis and polio booster vaccination in the danish vaccination register," *BMC Public Health*, vol. 20, no. 1, pp. 1–6, 2020. DOI:10.1186/s12889-020-09816-w

[14] C. E. Madubueze, K. A. Tijani, and Fatmawati, "A deterministic mathematical model for optimal control of diphtheria disease with booster vaccination," *Healthcare Analytics*, vol. 4, p. 100281, 2023. DOI:10.1016/j.health.2023.100281

[15] N. Rahmi and M. I. Pratama, "Model analysis of diphtheria disease transmission with vaccination, quarantine, and hand-washing behavior," *JTAM (Jurnal Teori dan Aplikasi Matematika)*, vol. 7, no. 2, pp. 462–474, 2023. DOI:10.31764/jtam.v7i2.13466

[16] N. Medugu *et al.*, "A review of the current diphtheria outbreaks," *African Journal of Clinical and Experimental Microbiology*, vol. 24, no. 2, pp. 120–129, 2023. DOI:10.4314/ajcem.v24i2.2

[17] E. S. Udofia *et al.*, "Age structured deterministic model of diphtheria infection," *Earthline Journal of Mathematical Sciences*, vol. 14, no. 3, pp. 391–404, 2024. DOI:10.34198/ejms.14324.391404

[18] F. Finger *et al.*, "Real-time analysis of the diphtheria outbreak in forcibly displaced myanmar nationals in bangladesh," *BMC Medicine*, vol. 17, pp. 1–11, 2019. DOI:10.1186/s12916-019-1288-7

[19] Z. Islam *et al.*, "Global stability analysis and parameter estimation for a diphtheria model: A case study of an epidemic in rohingya refugee camp in bangladesh," *Computational and Mathematical Methods in Medicine*, vol. 2022, pp. 1–13, 2022. DOI:10.1155/2022/6545179

[20] N. Izzati and A. Andriani, "Dynamical analysis of diphtheria epidemic model with natural immunity rate on exposed individuals," in *Journal of Physics: Conference Series*, vol. 1869, no. 1, p. 012117, 2021. DOI:10.1088/1742-6596/1869/1/012117

[21] N. Izzati, A. Andriani, and R. Robi'Aqolbi, "Optimal control of diphtheria epidemic model with prevention and treatment," in *Journal of Physics: Conference Series*, vol. 1663, no. 1, p. 012042. DOI:10.1088/1742-6596/1663/1/012042

[22] M. Grasse *et al.*, "Booster vaccination against tetanus and diphtheria: insufficient protection against diphtheria in young and elderly adults," *Immunity & Ageing*, vol. 13, pp. 1–9, 2016. DOI:10.1186/s12979-016-0081-0

[23] N. Abdulrasheed *et al.*, "Recurrent diphtheria outbreaks in nigeria: A review of the underlying factors and remedies," *Immunity, Inflammation and Disease*, vol. 11, no. 11, p. e1096, 2023. DOI:10.1002/iid3.1096

[24] F. Ilahi and A. Widiana, "The effectiveness of vaccine in the outbreak of diphtheria: Mathematical model and simulation," in *IOP Conference Series: Materials Science and Engineering*, vol. 434, no. 1, p. 012006, 2018. DOI:10.1088/1757-899X/434/1/012006

[25] S. Kanchanarat, S. Chinviriyasit, and W. Chinviriyasit, "Mathematical assessment of the impact of the imperfect vaccination on diphtheria transmission dynamics," *Symmetry*, vol. 14, no. 10, p. 2000, 2022. DOI:10.3390/sym14102000

[26] I. S. Fauzi *et al.*, "Assessing the impact of booster vaccination on diphtheria transmission: Mathematical modeling and risk zone mapping," *Infectious Disease Modelling*, vol. 9, no. 1, pp. 245–262, 2024. DOI:10.1016/j.idm.2024.01.004

[27] S. Adewale *et al.*, "Mathematical analysis of quarantine on the dynamical transmission of diphtheria disease," *International Journal of Science and Engineering Investigations*, vol. 6, no. 5, pp. 8–17, 2017.

[28] W. L. Conklin, "Clinical versus bacteriological diagnosis and quarantine of diphtheria," *Buffalo Medical Journal*, vol. 41, no. 9, p. 660, 1902.

[29] S. Withers, J. R. Ranson, and E. D. Humphrys, "Shortening the quarantine period for diphtheria convalescents and carriers," *Journal of the American Medical Association*, vol. 87, no. 16, pp. 1266–1269, 1926. DOI:10.1001/jama.1926.02680160014004

[30] R. Kurniati, S. Sugiarto, and S. Nurwijaya, "Dynamical system for tuberculosis outbreak with vaccination treatment and different interventions on the burden of drug resistance," *Jambura Journal of Biomathematics (JJBM)*, vol. 5, no. 1, pp. 10–18, 2024. DOI:10.37905/jjbm.v5i1.21903

[31] M. M. Ojo and E. F. Doungmo Goufo, "Assessing the impact of control interventions and awareness on malaria: a mathematical modeling approach," *Communications in Mathematical Biology and Neuroscience*, vol. 2021, pp. 1–31, 2021. DOI:10.28919/cmbn/6632

[32] Statista, "Population growth in nigeria from 2012 to 2022," 2022, https://www.statista.com/statistics/382235/population-growth-in-nigeria/, Accesed on 11 March 2025.

[33] Statista, "Population of nigeria in selected years between 1950 and 2023," 2023, https://www.statista.com/statistics/1122838/population-of-nigeria/, Accesed on 11 March 2025.

[34] Statista, "Life expectancy at birth in nigeria in 2023, by gender," 2023, https://www.statista.com/statistics/1122851/life-expectancy-in-nigeria-by-gender/ Accessed on 29 April 2025.

[35] N. KidsHealth, "Diphtheria," 2024, https://kidshealth.org/en/parents/, Accesed on 29 April 2025.

[36] J. Hallare and V. Gerriets, "Half life," *StatPearls*, 2020, Accessed on April 29, 2025.

[37] N. C. Marshall *et al.*, "Ten years of diphtheria toxin testing and toxigenic cutaneous diphtheria investigations in alberta, canada: A highly vaccinated population," in *Open Forum Infectious Diseases*, vol. 9, no. 1, p. ofab414, 2022. DOI:10.1093/ofid/ofab414

[38] A. M. Acosta *et al.*, "Diphtheria," *Epidemiology and Prevention of Vaccine-Preventable Diseases*, 2021.

[39] A. Abidemi, J. Akanni, and O. Makinde, "A non-linear mathematical model for analysing the impact of covid-19 disease on higher education in developing countries," *Healthcare Analytics*, vol. 3, p. 100193, 2023. DOI:10.1016/j.health.2023.100193

[40] M. O. Akinade and A. S. Afolabi, "Sensitivity and stability analyses of a lassa fever disease model with control strategies," *IOSR Journal of Mathematics (IOSR-JM)*, vol. 16, no. 1, pp. 29–42, 2020. DOI: 10.9790/5728-1601022942

[41] F. O. Akinpelu and R. Akinwande, "Mathematical model for lassa fever and sensitivity analysis," *Journal of Science and Engineering Research*, vol. 5, no. 6, pp. 1–9, 2018.

[42] E. Bakare and C. Nwozo, "Bifurcation and sensitivity analysis of malaria–schistosomiasis co-infection model," *International Journal of Applied and Computational Mathematics*, vol. 3, pp. 971–1000, 2017. DOI:10.1007/s40819-017-0394-5

[43] C. M. Veronica *et al.*, "Mathematical modeling and stability analyses on the transmission dynamics of bacterial meningitis," *Journal of Mathematics and Computer Science*, vol. 11, no. 6, pp. 7384–7413, 2021. DOI:10.28919/jmcs/6513

[44] E. Kanyi, A. S. Afolabi, and N. O. Onyango, "Optimal control analysis of schistosomiasis dynamics," *Journal of Mathematics and Computer Science*, vol. 11, no. 4, pp. 4599–4630, 2021. DOI:10.28919/jmcs/5847

[45] A. Abidemi, Fatmawati, and O. J. Peter, "An optimal control model for dengue dynamics with asymptomatic, isolation, and vigilant compartments," *Decision Analytics Journal*, p. 100413, 2024. DOI:10.1016/j.dajour.2024.100413

[46] I. Kour, L. Singhal, and V. Gupta, "*Diphtheria: A paradigmatic vaccine-preventable toxigenic disease with changing epidemiology*." in Recent Advances in Pharmaceutical Innovation and Research, pp. 749–759. Singapore: Springer, 2023. DOI:10.1007/978-981-99-2302-1_30

[47] M. Petráš *et al.*, "Factors influencing persistence of diphtheria immunity and immune response to a booster dose in healthy slovak adults," *Vaccines*, vol. 7, no. 4, p. 139, 2019. DOI:10.3390/vaccines7040139

[48] V. D. Bampoe *et al.*, "A review of adverse events from the use of diphtheria antitoxin (dat) in the united states, 2004–2019," *Clinical Infectious Diseases*, vol. 74, no. 11, pp. 2082–2083, 2022. DOI:10.1093/cid/ciab899

[49] B. L. Wiedermann, "Diphtheria in the 21st century: new insights and a wake-up call," *Clinical Infectious Diseases*, vol. 71, no. 1, pp. 98–99, 2020. DOI:10.1093/cid/ciz813

[50] A. Adikari and Y. Jayathunga, "Optimal control for resource allocation in a multi-patch epidemic model with human dispersal behavior," *Communication in Biomathematical Sciences*, vol. 8, no. 1, pp. 1–18, 2025. DOI:10.5614/cbms.2025.8.1.1

[51] A. B. Gumel and S. Lenhart, *Modeling Paradigms and Analysis of Disease Transmission Models*. in Providence, vol. 75. USA: American Mathematical Society, 2010.

[52] S. Lenhart and J. T. Workman, *Optimal control applied to biological models*. in Boca Raton. USA: Chapman and Hall/CRC, 2007, ISBN 978-1-58488-640-2.

[53] F. A. Oguntolu *et al.*, "Mathematical modeling on the transmission dynamics of diphtheria with optimal control strategies," *Jambura Journal of Biomathematics (JJBM)*, vol. 6, no. 1, pp. 1–22, 2025. DOI:10.37905/jjbm.v6i1.29716

[54] H. Alrabaiah *et al.*, "Optimal control analysis of hepatitis b virus with treatment and vaccination," *Results in Physics*, vol. 19, p. 103599, 2020. DOI:10.1016/j.rinp.2020.103599

[55] A. Altamirano-Fernández, A. Rojas-Palma, and S. Espinoza-Meza, "Existence of solutions for an optimal control problem in forestry management," in *Journal of Physics: Conference Series*, vol. 2515, no. 1, p. 012001, 2023. DOI:10.1088/1742-6596/2515/1/012001

[56] W. H. Fleming and R. W. Rishel, *Deterministic and Stochastic Optimal Control*. New York: Springer New York, 2012, ISBN:978-1-4612-6382-1. DOI:10.1007/978-1-4612-6380-7

[57] O. D. Falowo, S. Olaniyi, and A. T. Oladipo, "Optimal control assessment of rift valley fever model with vaccination and environmental sanitation in the presence of treatment delay," *Modeling Earth Systems and Environment*, vol. 9, no. 1, pp. 457–471, 2023. DOI:10.1007/s40808-022-01508-1

[58] E. E. Joshua, E. T. Akpan, and U. G. Inyang, "Computational nonlinear dynamics: Analysis and assessment in optimal control of covid-19 in akwa ibom state, nigeria," *Journal of Advances in Mathematics and Computer Science*, vol. 39, no. 1, pp. 1–19, 2024. DOI:10.9734/jamcs/2024/v39i11858

[59] H. R. Joshi, "Optimal control problems in PDE and ODE systems [Dissertation]," in Knoxville. USA: The University of Tennessee, 2002.

[60] F. Agusto and M. C. A. Leite, "Optimal control and cost-effective analysis of the 2017 meningitis outbreak in nigeria," *Infectious Disease Modelling*, vol. 4, pp. 161–187, 2019. DOI:10.1016/j.idm.2019.05.003

[61] L. J. Allen *et al.*, "*Mathematical Epidemiology*." in Berlin. Germany: Springer, 2008.

[62] F. Brauer *et al.*, "*Mathematical Models in Epidemiology*," Cham. Switzerland: Springer, 2019.

[63] J. K. K. Asamoa *et al.*, "Optimal control and comprehensive cost-effectiveness analysis for covid-19," *Results in Physics*, vol. 33, p. 105177, 2022. DOI:10.1016/j.rinp.2022.105177

[64] F. S. García, "Mathematical modeling approaches in epidemiology: within-host dynamics, control strategies and cost-effectiveness analysis [Dissertation]," in Centro de Investigación en Matemáticas. Mexico: Guanajuato, 2020.

[65] S. Olaniyi *et al.*, "Efficiency and economic analysis of intervention strategies for recurrent malaria transmission," *Quality & Quantity*, vol. 58, no. 1, pp. 627–645, 2024. DOI:10.1007/s11135-023-01664-1

[66] B. E. Nichols *et al.*, "Cost-effectiveness analysis of pre-exposure prophylaxis for hiv-1 prevention in the netherlands: a mathematical modelling study," *The Lancet Infectious Diseases*, vol. 16, no. 12, pp. 1423–1429, 2016. DOI:10.1016/S1473-3099(16)30311-5

[67] D. Aldila *et al.*, "On the role of early case detection and treatment failure in controlling tuberculosis transmission: A mathematical modeling study," *Communication in Biomathematical Sciences*, vol. 7, no. 1, pp. 61–86, 2024. DOI:10.5614/cbms.2024.7.1.4

[68] H. A. Fatahillah and D. Aldila, "Forward and backward bifurcation analysis from an imperfect vaccine efficacy model with saturated treatment and saturated infection," *Jambura Journal of Biomathematics (JJBM)*, vol. 5, no. 2, pp. 132–143, 2024. DOI:10.37905/jjbm.v5i2.28810

[69] A. Abidemi and O. J. Peter, "Deterministic double dose vaccination model of covid-19 transmission dynamics–optimal control strategies with cost-effectiveness analysis," *Communication in Biomathematical Sciences*, vol. 7, no. 1, pp. 1–33, 2024. DOI:10.5614/cbms.2024.7.1.1

[70] F. B. Agusto and I. M. ELmojtaba, "Optimal control and cost-effective analysis of malaria/visceral leishmaniasis co-infection," *PLOS ONE*, vol. 12, no. 2, p. e0171102, 2017. DOI:10.1371/journal.pone.0171102

[71] R. Boucekkine and T. Loch-Temzelides, "Introduction to the special issue on mathematical economic epidemiology models," *Economic Theory*, vol. 77, no. 1–2, pp. 1–7, 2024. DOI:10.1007/s00199-023-01541-w

[72] E. J. Dasbach, E. H. Elbasha, and R. P. Insinga, "Mathematical models for predicting the epidemiologic and economic impact of vaccination against human papillomavirus infection and disease," *Epidemiologic Reviews*, vol. 28, no. 1, pp. 88–100, 2006. DOI:10.1093/epirev/mxj006

[73] P. J. White, "*nfectious Diseases (Fourth Edition)*," in 5 - Mathematical models in infectious disease epidemiology, pp. 49–53.e1. Elsevier, 2017. DOI:10.1016/B978-0-7020-6285-8.00005-8

[74] Y. A. Adi, N. Irsalinda, and M. Z. Ndii, "Optimal control and cost-effectiveness analysis in an epidemic model with viral mutation and vaccine intervention," *CAUCHY: Jurnal Matematika Murni dan Aplikasi*, vol. 7, no. 2, pp. 173–185,

2022. DOI:10.18860/ca.v7i2.13184

[75] D. Angulo *et al.*, "Fine-grained mathematical modeling for cost-effectiveness evaluation of public health policies for cervical cancer, with application to a colombian case study," *BMC Public Health*, vol. 23, no. 1, p. 1470, 2023. DOI:10.1186/s12889-023-16022-x

[76] P. Asplin *et al.*, "Epidemiological and health economic implications of symptom propagation in respiratory pathogens: A mathematical modelling investigation," *PLOS Computational Biology*, vol. 20, no. 5, p. e1012096, 2024. DOI:10.1371/journal.pcbi.1012096

[77] H. Bang and H. Zhao, "Average cost-effectiveness ratio with censored data," *Journal of Biopharmaceutical Statistics*, vol. 22, no. 2, pp. 401–415, 2012. DOI:10.1080/10543406.2010.544437

[78] S. Kim *et al.*, "The epidemiologic and economic impact of varicella and herpes zoster vaccination in south korea: A mathematical modelling study," *Vaccine*, vol. 42, no. 19, pp. 4046–4055, 2024. DOI:10.1016/j.vaccine.2024.05.016

[79] K. N. Wanis *et al.*, "Health and economic impact of intensive surveillance for distant recurrence after curative treatment of colon cancer: A mathematical modeling study," *Diseases of the Colon & Rectum*, vol. 62, no. 7, pp. 872–881, 2019. DOI:10.1097/DCR.0000000000001364